Proceedings of the Mini-Workshop

Quark Masses and Hadron Spectra

Bled, Slovenia, July 6 – 13, 2014

Edited by

Bojan Golli

Mitja Rosina

Simon Širca

University of Ljubljana and Jožef Stefan Institute

The Mini-Workshop *Quark Masses and Hadron Spectra*

Organizing Committee

Mitja Rosina, Bojan Golli, Simon Širca

List of participants

Borut Bajc, Ljubljana, `borut.bajc@ijs.si`
Marko Bračko, Ljubljana, `marko.bracko@ijs.si`
Thomas Cohen, Maryland, `cohen@physics.umd.edu`
Harald Fritzsch, Munich, `fritzch@mppmu.mpg.de`
Bojan Golli, Ljubljana, `bojan.golli@ijs.si`
Brigitte Hiller, Coimbra, `brigitte@fis.uc.pt`
Dubravko Klabučar, Zagreb, `klabucar@oberon.phy.hr`
Regina Kleinhappel, Graz, `regina.kleinhappel@uni-graz.at`
Luka Leskovec, Ljubljana, `luka.leskovec@ijs.si`
Debora Menezes, Florianopolis, `debora.p.m@ufsc.br`
Miha Nemevšek, Ljubljana, `miha.nemevsek@ijs.si`
Markus Pak, Graz, `markus.pak@uni-graz.at`
Willi Plessas, Graz, `willibald.plessas@uni-graz.at`
Bogdan Povh, Heidelberg, `b.povh@mpi-hd.mpg.de`
Saša Prelovšek, Ljubljana, `Sasa.Prelovsek@ijs.si`
Mitja Rosina, Ljubljana, `mitja.rosina@ijs.si`
Simon Širca, Ljubljana, `simon.sirca@fmf.uni-lj.si`

Contents

Preface

This year, the relation between the structure of constituent quarks and the corresponding hadron spectra was exciting many lively discussions. Can a constituent quark containing a pion cloud, for example, explain the ratio between the Λ-nucleus and N-nucleus potential or the width of baryons? Constituent quarks are of course a model-dependent concept and their masses depend on whether the model is relativistic or not. However, the difference between the constituent mass and the current mass is almost constant from light to heavy quarks. This amazing fact may reveal the clue to the dominant mechanisms of dynamical mass generation. The generation of constituent-quark masses can be followed nicely also in the Dyson-Schwinger approach.

The progress in the NJL model has shown the importance of three- and four-quark interactions, interesting features of the QCD phase diagram and how current quark masses can be determined consistently. Particularly interesting is the effect of vector-vector interactions and of the magnetic field on the equation of state, consistent with the two-solar-mass stars.

Search for tetraquarks in normal and exotic spectra is still inconclusive, both experimentally and theoretically. Evidence is accumulating.

The old idea of composite weak bosons has been revived by the measurable prediction that the 126 GeV resonance might be a S' excitation of the Z^0 rather than a Higgs if experiments find a strong enhancement of the $\gamma\gamma$ decay.

Even the constituent quark model fans were eagerly listening to the progress in Lattice QCD, as a comparison with their results. Examples are the positive parity D_s mesons and Z_c^+. Recent assignments of quantum numbers in the quarkonium(-like) spectroscopy at Belle and fresh puzzles might guide new model calculations.

Again, the traditional experimental talks will motivate several studies for the next Bled Workshops! The nuclear few-body problem is still alive; the role of S'- and D-states appears in the spin structure of ^{3}He studied by deuteron and nucleon knock-out pocesses.

There are so many open problems which require relaxed and open-minded discussions. It is just for this purpose that we intend to continue our traditional hadronic workshops also in future.

Ljubljana, November 2014   B. Golli, M. Rosina, S. Širca

Predgovor

Letos smo živahno razpravljali o povezavi med strukturo oblečenih kvarkov in ustreznimi hadronskimi spektri. Ali lahko, na primer, kvark oblečen v mezonski oblak razloži razmerje med potencialoma nukleon-jedro ter Λ-jedro, ali pa širine barionov? Oblečeni kvarki so sicer od modela odvisen pojem in njihove mase so odvisne tudi od upoštevanja relativnosti. Vendar je razlika med oblečeno in golo maso skoraj konstantna od lahkih do težkih kvarkov. To presenetljivo dejstvo bo morda osvetlilo, kateri je glavni mehanizem za dinamično tvorbo mas. Tudi pristop z Dyson-Schwingerjevo enačbo je perspektiven za ta namen.

Napredek pri modelu Nambuja in Jona-Lasinia je pokazal, da so važne interakcije med tremi in štirimi kvarki, poglobil je razumevanje kromodinamskega faznega diagrama in omogočil dosledno izpeljavo golih mas kvarkov. Zelo zanimiv je učinek vektorske interakcije in magnetnega polja na enačbo stanja, ki je potem v skladu z odkritjem zvezd z dvojno maso Sonca.

Iskanje tetrakvarkov v normalnih in v eksotičnih spektrih še vedno ni prepričljivo, niti eksperimenalno niti teoretično. Podpora pa narašča.

Staro zamisel, da so šibki bozoni sestavljeni, je poživila napoved, da bi se dalo eksperimentalno razlikovati, ali je resonanca pri 126 GeV vzbujeno stanje Z^0 ali Higgsov bozon. Pri prvem bi bila namreč mnogo večja verjetnost za razpad v dva gama.

Celo pristaši modelov z oblečenimi kvarki so radi poslušali o napredku pri kromodinamiki na mreži, za primerjavo z njihovimi rezultati. Lep zgled so mezoni D_s s pozitivno parnostjo ter Z_c^+. Nedavne določitve kvantnih števil pri kvarkonijih in "kvarkonijih" v laboratoriju Belle in sveže uganke utegnejo vzpodbuditi nove modelske račune.

Spet pričakujemo, da bodo tradicionalni eksperimentalni prikazi vzpodbudili študije za naslednjo Blejsko delavnico! Tudi jedrski problem treh teles je še živ; pri spinski strukturi ^{3}He je pokazalo izbijanje devterona in nukleona znatno vlogo stanj S' in D.

Mnogo je odprtih problemov, ki zahtevajo sproščeno in prostodušno debato. Prav v ta namen nameravamo nadaljevati naše tradicionalna hadronske delavnice tudi v bodoče.

Ljubljana, november 2014 B. Golli, M. Rosina, S. Širca

Workshops organized at Bled

▷ *What Comes beyond the Standard Model*
    (June 29–July 9, 1998), Vol. **0** (1999) No. 1
    (July 22–31, 1999)
    (July 17–31, 2000)
    (July 16–28, 2001), Vol. **2** (2001) No. 2
    (July 14–25, 2002), Vol. **3** (2002) No. 4
    (July 18–28, 2003) Vol. **4** (2003) Nos. 2-3
    (July 19–31, 2004), Vol. **5** (2004) No. 2
    (July 19–29, 2005) , Vol. **6** (2005) No. 2
    (September 16–26, 2006), Vol. **7** (2006) No. 2
    (July 17–27, 2007), Vol. **8** (2007) No. 2
    (July 15–25, 2008), Vol. **9** (2008) No. 2
    (July 14–24, 2009), Vol. **10** (2009) No. 2
    (July 12–22, 2010), Vol. **11** (2010) No. 2
    (July 11–21, 2011), Vol. **12** (2011) No. 2
    (July 9–19, 2012), Vol. **13** (2012) No. 2
    (July 14–21, 2013), Vol. **14** (2013) No. 2
    (July 20–28, 2014), Vol. **15** (2014) No. 2
▷ *Hadrons as Solitons* (July 6–17, 1999)
▷ *Few-Quark Problems* (July 8–15, 2000), Vol. **1** (2000) No. 1
▷ *Statistical Mechanics of Complex Systems* (August 27–September 2, 2000)
▷ *Selected Few-Body Problems in Hadronic and Atomic Physics* (July 7–14, 2001),
    Vol. **2** (2001) No. 1
▷ *Studies of Elementary Steps of Radical Reactions in Atmospheric Chemistry*
    (August 25–28, 2001)
▷ *Quarks and Hadrons* (July 6–13, 2002), Vol. **3** (2002) No. 3
▷ *Effective Quark-Quark Interaction* (July 7–14, 2003), Vol. **4** (2003) No. 1
▷ *Quark Dynamics* (July 12–19, 2004), Vol. **5** (2004) No. 1
▷ *Exciting Hadrons* (July 11–18, 2005), Vol. **6** (2005) No. 1
▷ *Progress in Quark Models* (July 10–17, 2006), Vol. **7** (2006) No. 1
▷ *Hadron Structure and Lattice QCD* (July 9–16, 2007), Vol. **8** (2007) No. 1
▷ *Few-Quark States and the Continuum* (September 15–22, 2008),
    Vol. **9** (2008) No. 1
▷ *Problems in Multi-Quark States* (June 29–July 6, 2009), Vol. **10** (2009) No. 1
▷ *Dressing Hadrons* (July 4–11, 2010), Vol. **11** (2010) No. 1
▷ *Understanding hadronic spectra* (July 3–10, 2011), Vol. **12** (2011) No. 1
▷ *Hadronic Resonances* (July 1–8, 2012), Vol. **13** (2012) No. 1
▷ *Looking into Hadrons* (July 7–14, 2013), Vol. **14** (2013) No. 1
▷ *Quark Masses and Hadron Spectra* (July 6–13, 2014), Vol. **15** (2014) No. 1

Tetraquarks and Large N_c QCD

Thomas D. Cohen

Department of Physics, University of Maryland, College Park, MD 20742-4111

Search for tetraquarks in normal and exotic spectra is still inconclusive, both experimentally and theoretically. Evidence is accumulating. The question has been discussed whether bound tetraquarks can exist in the large N_c limit. They can exist in an interesting antisymmetric variant of QCD.

Composite Weak Bosons at the LHC

Harald Fritzsch

Department für Physik Ludwig-Maximilians-Universität München, Germany

Abstract. In a composite model of the weak bosons the excited bosons, in particular the p-wave bosons, are studied. The state with the lowest mass is identified with the boson, which has been discovered recently at the "Large Hadron Collider" at CERN. Specific properties of the excited weak bosons are studied, in particular their decays into weak bosons and into photons.

In the Standard Model of the electroweak interactions the masses of the weak bosons and of the leptons and quarks are generated by a spontaneous breaking of the electroweak symmetry. Besides the weak bosons a scalar boson must exist ("Higgs boson"). Recently one has discovered a new scalar boson with a mass of about 126 GeV (ref.(1,2)), which might be the Higgs boson.

Here I discuss the possibility that the weak bosons are composite particles. The new scalar boson, observed at the LHC, would be an excited Z-boson.

In the Standard Theory the masses of the weak bosons, leptons and quarks are generated by the spontaneous symmetry breaking. A doublet of scalar fields is introduced, which breaks the weak isospin symmetry spontaneously and develops a non-zero vacuum expectation valus. The weak bosons absorb three of the four scalar fields and obtain a mass, which is proportional to the vacuum expectation value. The remaining neutral scalar boson is the "Higgs" boson.

In QCD the three ρ-mesons are degenerate in mass, if the electromagnetic interaction is switched off and the two light quark masses are zero. Once the electromagnetic interaction is introduced, the charged mesons receive an additional small contribution to the mass, which is due to the Coulomb self energy. In addition the neutral ρ-meson mixes with the photon and its mass increases. This mass shift can be calculated. It depends on a mixing parameter μ, which is determined by the electric charge, the decay constant F_ρ and the mass of the ρ-meson:

$$\mu = e \frac{F_\rho}{M_\rho} .$$ (1)

The mass shift due to the mixing is given by:

$$M_{\rho^0}^2 = M_{\rho^+}^2 \left(\frac{1}{1 - \mu^2} \right) .$$ (2)

The decay constant is measured to about 220 MeV - it is about equal to the QCD scale parameter Λ_c. One obtains $\mu \approx 0.09$ - it leads to a mass shift of about 3 MeV.

We assume that the weak bosons are composite particles. They consist of a lefthanded fermion and its antiparticle, which are denoted as "haplons". A theory of this type was proposed in 1981 (see ref.(3) and ref.(4,5,6,7,8)). The new confining chiral gauge theory is denoted as QHD. The QHD mass scale is given by a mass parameter Λ_h, which determines the size of the weak bosons. The haplons interact with each other through the exchange of massless gauge bosons.

Two types of haplons are needed as constituents of the weak bosons, denoted by α and β. Their electric charges in units of e are:

$$h = \begin{pmatrix} +\frac{1}{2} \\ -\frac{1}{2} \end{pmatrix} . \tag{3}$$

The three weak bosons have the following internal structure:

$$
\begin{aligned}
W^+ &= \overline{\beta}\alpha , \\
W^- &= \overline{\alpha}\beta , \\
W^3 &= \frac{1}{\sqrt{2}} \left(\overline{\alpha}\alpha - \overline{\beta}\beta \right) .
\end{aligned}
\tag{4}
$$

In the absence of electromagnetism the weak bosons are degenerate in mass. If the electromagnetic interaction is introduced, the mass of the neutral boson increases due to the mixing with the photon (ref. (9,10)).

In the Standard Theory the mixing is generated by the scalar fields. Both the photon and the Z-boson are mixtures of the $SU(2)$ and $U(1)$ gauge bosons. Here the mixing is a dynamical mixing, analogous to the mixing of ρ - mesons. It is described by the mixing parameter m, determined by the decay constant of the weak boson:

$$m = e\frac{F_W}{M_W} . \tag{5}$$

One finds for the mass difference beween the charged and the neutral weak boson:

$$M_Z^2 = M_{W^+}^2 \left(\frac{1}{1-m^2} \right) . \tag{6}$$

In the standard electroweak theory there is a similar equation - the mixing parameter m must be replaced by $\sin\theta_w$. According to the experiments the mixing parameter m is about 0.485, i. e. about five times larger than the mixing paramter for the ρ-mesons. Using the experimental value, one can determine the decay constant for the weak bosons:

$$F_W \approx 125 \text{ GeV}. \tag{7}$$

As in QCD it is expected that the decay constant of the weak boson and the QHD mass scale are related. The decay constant of the ρ-meson and the QCD

mass scale are about the same - in QHD the weak decay constant and Λ_h should be of the same order of magnitude. Details will depend in particular on the gauge group of QHD. We expect that Λ_h is in the range between 0.12 TeV and 1 TeV.

The weak bosons consist of pairs of haplons, which are in an s-wave. The spins of the two haplons are aligned, as the spins of the quarks in a ρ-meson. The first excited states are those, in which the two haplons are in a p-wave. We describe the quantum numbers of these states by $I(J)$. The $SU(2)$-representation is denoted by I - the symbol J describes the total angular momentum. There are three $SU(2)$ singlets, which we denote by S(0), S(1) and S(2), and three triplet states, denoted by T(0), T(1) and T(2).

The boson S(0) is the particle, which has been observed at CERN (ref. (1,2)):

$$M(S(0)) = 126 \text{ GeV.} \tag{8}$$

In analogy to QCD we expect that the masses of the other p-wave states are in the range 0.3 - 0.5 TeV. The mass of the S(1) - boson should be just above 0.3 TeV, the mass of the S(2) - boson between 0.4 and 0.5 TeV.

The masses of the $SU(2)$ - triplet bosons T should be larger than the masses of the S - bosons. We compare the spectrum of these bosons with the spectrum of the corresonding mesons in QCD. Thus the mass of the T(0) - boson should be about 0.3 TeV, the mass of the T(1) - boson just above 0.4 TeV, and the mass of the T(0) - boson should be in the range 0.5 - 0.6 TeV.

The S(0) - boson will decay mainly into two charged weak bosons or into two Z-bosons (one of them virtual respectively), into a photon and a Z-boson and into two photons. The Z-boson is the boson W^3, mixed with the photon. The mixing angle is the weak angle, measured to about 28.7 degrees. Using this angle, we can calculate the branching ratios BR for the various decays, taking into accoutn phase space corrections. The branching ratio for the decay into charged weak bosons is denoted by B.

$$S(0) \Longrightarrow (\text{"}W\text{"} + W) \qquad BR = B,$$

$$S(0) \Longrightarrow (\text{"}Z\text{"} + Z) \qquad BR \approx 0.55 \text{ B},$$

$$S(0) \Longrightarrow (Z + \gamma) \qquad BR \approx 0.04 \text{ B},$$

$$S(0) \Longrightarrow (\gamma + \gamma) \qquad Br \approx 0.05 \text{ B}.$$

We would not expect that the decay rates for the decays of S(0) into letons and quarks are given by the mass of the fermion, as they are for the Higgs boson. The branching ratios for the decays into an electron pair, into a muon pair, into a tau pair or into a neutrino pair should be similar. The decay of the S(0) into a muon pair could be observed in the near future at the LHC.

The bosons S(1) and S(2) have a much higher mass as the S(0) - boson. They will decay mainly into three or four weak bosons. The $SU(2)$ - triplet bosons T(0), T(1) and T(2) will decay mainly into four or five weak bosons or photons. Decays

into two weak bosons, a weak boson and a photon or two photons are strongly suppressed.

The properties of the new boson, which has been discovered at the LHC, should be investigated in detail. If the model, discussed here, is correct and the new boson is the state $S(0)$, the other excited bosons $S(1)$, $S(2)$ and $T(0)$ should be discovered soon at the LHC.

References

1. Atlas collaboration:
   arXiv:1202.1414,arXiv:1202.1408, arXiv:1202.1415.
2. CMS collaboration:
   arXiv:1202.1488, arXiv:1202.1489, arXiv:1202.1487.
3. H. Fritzsch and G. Mandelbaum, Phys. Lett. B102 (1981) 319;
   Phys. Lett. B 109 (1982) 224.
4. R. Barbieri, R. Mohapatra and A. Masiero, Phys. Lett. B 105 (1981) 369.
5. H. Fritzsch. D. Schildknecht and R. Kogerler, Phys. Lett. B 114 (1982) 157.
6. L. F. Abbott and E. Farhi, Phys. Lett. B 101, 69 (1981).
7. T. Kugo, S. Uehara and T. Yanagida, Phys. Lett. B 147, 321 (1984).
8. S. Uehara and T. Yanagida, Phys. Lett. B 165, 94 (1985).
9. H. Fritzsch, arXiv:1201.2512
10. H. Fritzsch, Mod. Phys. Lett. A26, 2305 (2011)

Effective Lagrangian approach to multi-quark interactions⋆

A. A. Osipov, B. Hiller, A. H. Blin

Centro de Física Computacional, Departamento de Física da Universidade de Coimbra, 3004–516 Coimbra, Portugal

Abstract. In this workshop we have presented the results obtained in the three-flavour ($N_f = 3$) Nambu–Jona-Lasinio model Lagrangian which includes all non-derivative vertices at NLO in the $1/N_c$ expansion of spin zero multi-quark interactions. In particular the role played by the explicit chiral symmetry breaking interactions has been discussed in comparison with previous model Lagrangians.

The subject of this year's Bled workshop is "Quark masses and hadron spectra". The understanding of the origin of masses from fundamental principles may have moved a step closer with the announcement of the existence of the Higgs, however the reason for the hierarchy of masses observed for several families of leptons and quarks still eludes us. The current quark masses are external to the gauge principle underlying the foundations of QCD. In an effective approach to QCD the most innocuous way is to consider them born from external sources interacting with originally massless fields which comply with all the symmetries. If in addition the study of strong interactions is limited to the energy range which is of order $\Lambda \simeq 4\pi f_\pi \sim 1$ GeV [1], where Λ characterizes the scale for spontaneous chiral symmetry χ_S breaking, a firm set-up for its systematic inclusion is supplied by the seminal papers of Nambu and Jona-Lasinio (NJL) [2].

Our procedure relies on the very general assumption that this scale determines the hierarchy of local multi-quark interactions which model QCD at low energies. It has been pointed out in [3,4] that it is sufficient to truncate the tower of multi-quark interactions at 8 quarks (q) to complete in 4D the number of vertices relevant at the scale of dynamical chiral symmetry breaking.

The $U(1)_A$ symmetry breaking 't Hooft ($2N_f$) flavor determinant [5,6] adds $1/N_c$ suppressed interactions to the original NJL Lagrangian [7,8]. Having first focussed on the resolution of the instability of this model's effective potential [9], we have enlarged the Lagrangian by a general set of equally suppressed spin zero 8q interactions [10,11].

Later on, showing that the N_c counting rules are congruent with the classification of vertices in terms of the χ_S breaking scale, we have taken into consideration the terms of higher order in the current quark-mass expansion [12,13],

---

⋆ Talk delivered by B. Hiller

which are responsible for the explicit chiral symmetry breaking at the same order as the 't Hooft determinant and eight quark terms previously analyzed. The standard mass term of the free Lagrangian is only a part of the more complicated picture arising in effective models beyond leading order [14]. Chiral perturbation theory [15–17] gives a well-known example of a self consistent accounting of the mass terms, order by order, in an expansion in the masses themselves.

Using path integral bosonization techniques which take appropriately into account the quark mass differences [18, 19], the mesonic Lagrangian up to three-point mesonic vertices is obtained in [13].

We end up with $4 + 10 = 14$ low-energy constants at leading and NLO of the effective $1/N_c$ expansion. The model parameters are fully controlled on the theoretical side by symmetry arguments and on the experimental side by the characteristics of the low lying pseudoscalars and scalars. The number of observables described until now by far surpasses the number of parameters [13].

The tree level bosonized Lagrangian carries either signatures of violation of the Zweig-rule or of admixtures of $q^2 \bar{q}^2$ to the quark-antiquark states. Elsewhere these are obtained by considering explicitly meson loop corrections, tetraquark configurations and so on [20–31].

By calculating the mass spectra and the strong decays of the scalars, one can realize which multi-quark interactions are most relevant at the scale of spontaneous χ_S breaking. On the other hand, by analyzing the two photon radiative decays, where a different scale, associated with the electromagnetic interaction, comes into play, one can study the possible recombinations of quarks inside the hadron.

Our main results are so far:

1. We achieve total agreement with the empirical low lying pseudoscalar meson spectrum. The current quark mass dependent interaction terms mainly responsible for the fit belong to the class of OZI-violating interactions, representing additional corrections to the 't Hooft $U_A(1)$ breaking mechanism. Explicit χ_S breaking effects in interactions are essential to obtain the empirical ordering $m_K < m_\eta$ and the magnitude of the splitting. The fit of the $\eta - \eta'$ mass splitting together with the overall successful description of the whole set of low-energy pseudoscalar characteristics is actually a solution for a long standing problem of NJL-type models.

2. We are also capable to describe the spectrum of the light scalar nonet. The explicit χ_S breaking terms related with $q^2 \bar{q}^2$ admixtures are the main source of the fit associated with the empirical ordering $m_{\kappa_0} < m_{a_0} \sim m_{f_0}$. On the other hand, the mixing angle of the singlet-octet scalar states θ_S as well as the mass of the σ meson are strongly affected by OZI-violating short range forces.

3. With all parameters of the model fixed by the spectra we analyzed a bulk of two body decays at tree level of the bosonic Lagrangian: the strong decays of the scalars $\sigma \to \pi\pi$, $f_0(980) \to \pi\pi$, $\kappa(800) \to \pi K$, $a_0(980) \to \pi\eta$, as well as the two photon decays of $a_0(980)$, $f_0(980)$ and σ mesons and the anomalous decays of the pseudoscalars $\pi \to \gamma\gamma$, $\eta \to \gamma\gamma$ and $\eta' \to \gamma\gamma$.

Our results for the strong decays of the scalars are within the current expectations. The radiative decays of the scalars are smaller than the observed values for the $f_0(980)$ and the σ, but reasonable for the a_0.

We obtain that the $a_0(980)$ meson couples with a large strength of the multiquark components to the two kaon channel in its strong decay to two pions, but evidences a dominant $q\bar{q}$ component in its radiative decay. As opposed to this, the σ and $f_0(980)$ mesons do not display an enhanced $q\bar{q}$ component neither in their two photon decays nor in the strong decays. The widths of the $a_0(980) \to \pi\eta$ and $f_0(980) \to \pi\pi$ decays are well accomodated within a Flatté description. We corroborate other model calculations in which the coupling of the $f_0(980)$ and $a_0(980)$ mesons to the $K\bar{K}$ channel is needed for the description of the decays $f_0(980) \to \pi\pi$ and $a_0(980) \to \pi\eta$. We find that this coupling is most crucial for the latter process.

The radiative decays of the scalar mesons into two photons show that the main channel for the $a_0(980)$ decay proceeds through coupling to a $q\bar{q}$ state, while the radiative decays of singlet-octet states σ, f_0 must proceed through more complex strutures. This does not mean that the a_0 meson is mainly a $q\bar{q}$ state, but that the multi-quark component with the large strength in the two kaon channel, important for the reduction of the $a_0\pi\eta$ strong decay width, is not the leading process in the two photon decay of this meson.

Finally, the radiative decays of the pseudoscalars are in very good agreement with data.

4. The response to the external parameters T, μ has been recently addressed in [32], with implications on strange quark matter formation. In the early version of the model Lagrangian without the explicit NLO χ_S breaking terms one obtains that although the vacuum properties remain almost insensitive to the 8q interactions, their effects are remarkable for medium and thermal properties [33–38], as well as in presence of a strong constant magnetic field [39–42].

References

1. A. Manohar, H. Georgi, Nucl. Phys. B **234**, 189 (1984).
2. Y. Nambu, G. Jona-Lasinio, Phys. Rev. **122**, 345 (1961); **124**, 246 (1961).
3. A. A. Andrianov, V. A. Andrianov, Theor. Math. Phys. **94**, 3 (1993).
4. A. A. Andrianov, V. A. Andrianov, Int. J. of Mod. Phys. A **8**, 1981 (1993).
5. G. 't Hooft, Phys. Rev. D **14**, 3432 (1976).
6. G. 't Hooft, Phys. Rev. D **18**, 2199 (1978).
7. V. Bernard, R. L. Jaffe, U.-G. Meißner, Phys. Lett. B **198**, 92 (1987).
8. H. Reinhardt and R. Alkofer, Phys. Lett. B **207**, 482 (1988).
9. A. A. Osipov, B. Hiller, V. Bernard, A. H. Blin, Ann. of Phys. **321**, 2504 (2006).
10. A. A. Osipov, B. Hiller, J. da Providência, Phys. Lett. B **634**, 48 (2006).

11. A. A. Osipov, B. Hiller, A. H. Blin, J. da Providência, Ann. of Phys. **322**, 2021 (2007).
12. A. A. Osipov, B. Hiller, A. H. Blin, Eur. Phys. J. A **49**, 14 (2013).
13. A. A. Osipov, B. Hiller, A. H. Blin, Phys. Rev. D **88**, 054032 (2013).
14. J. Gasser, H. Leutwyler, Phys. Rep. **87**, 77 (1982).
15. S. Weinberg, Physica A **96**, 327 (1979).
16. H. Pagels, Phys. Rev. C **16**, 219 (1975).
17. J. Gasser, H. Leutwyler, Ann. of Phys. **158**, 142 (1984).
18. A. A. Osipov, B. Hiller, Phys. Lett. B **515**, 458 (2001).
19. A. A. Osipov, B. Hiller, Phys. Rev. D **64**, 087701 (2001).
20. R. J. Jaffe, Phys. Rev. D **15**, 267 (1977); R. J. Jaffe, Phys. Rev. D **15**, 281 (1977).
21. D. Black, A. H. Fariborz, E. Sannino, J. Schechter, Phys. Rev. D **59**, 074026 (1999).
22. D. Wong, K. F. Liu, Phys. Rev. D **21**, 2039 (1980)
23. S. Narrison, Phys. Lett. B **175**, 88 (1986).
24. E. van Beveren, T. A. Rijken, K. Metzger, C. Dullemond, G. Rupp, J. E. Ribeiro, Zeit. Phys. C **30**, 615 (1986).
25. J.I. Latorre, P. Pascoal, J. Phys. G **11**, L231 (1985)
26. M. Alford, R. L. Jaffe, Nucl. Phys. B **509**, 312 (1998)
27. N. N. Achasov, S. A. Devyanin, D. N. Shestakov, Z. Phys. C **16**, 55 (1984)
28. N. Isgur, J. Weinstein, Phys. Rev. D **41**, 2236 (1990).
29. A. H. Fariborz, R. Jora, J. Schechter, Phys. Rev. D **77**, 094004 (2008).
30. F. E. Close, N. A. Törnqvist, J. Phys. G: Nucl. Part. Phys. **28**, R249 (2002).
31. E. Klempt, A. Zaitsev, Phys. Rep. **454**, 1 (2007).
32. J. Moreira, J. Morais, B. Hiller, A.A. Osipov, A.H. Blin, arXiv:1409.0336 [hep-ph]
33. A. A. Osipov, B. Hiller, J. Moreira, A.H. Blin, J. da Providencia, Phys. Lett. B **646**, 91 (2007).
34. A. A. Osipov, B. Hiller, J. Moreira, A.H. Blin, Phys. Lett. B **659**, 270 (2008).
35. K. Kashiwa, H. Kouno, T. Sakaguchi, M. Matsuzaki, M. Yahiro, Phys. Lett. B **647**, 446 (2007);
36. K. Kashiwa, H. Kouno, M. Matsuzaki, M. Yahiro, Phys. Lett. B 662, 26 (2008).
37. B. Hiller, J. Moreira, A. A. Osipov, A.H. Blin, Phys. Rev. D **81**,116005 (2010).
38. A. Bhattacharyya, P. Deb, S. K. Ghosh, R. Ray, Phys. Rev. D **82** (2010) 014021
39. A. A. Osipov, B. Hiller, A. H. Blin, J. da Providência, Phys. Lett. B **650** 262 (2007).
40. R. Gatto, M. Ruggieri, Phys. Rev. D **82**, 054027 (2010).
41. R. Gatto, M. Ruggieri, Phys. Rev. D **83**, 034016 (2011).
42. M. Frasca, M. Ruggieri, Phys. Rev. D **83**, 094024 (2011).

Quark matter in strong magnetic fields

Débora Peres Menezes

Universidade Federal de Santa Catarina, Departamento de Física–CFM–CP 476, Campus Universitário–Trindade, CEP 88040-900, Florianópolis–SC, Brazil

Abstract. In the present work we are interested in understanding various properties of quark matter described by the Nambu-Jona-Lasinio (NJL) model once it is subject to strong magnetic fields. We start by analysing the possible different phase diagram structures. Secondly, we investigate the differences arising from different vector interactions in the Lagrangian densities and apply the results to stellar matter. We then look at deconfinement and chiral restauration properties at zero chemical potential with the (entagled) Polyakov NJL models. Finally, we investigate the position of the critical end point for different chemical potential and density scenarios.

1 Motivation and Results

The study of the QCD phase diagram, when matter is subject to strong external magnetic fields has been a topic of intense investigation recently. The fact that magnetic fields can reach intensities of the order of $B \sim 10^{19}$ G or higher in heavy-ion collisions [1] and up to 10^{18} G in the center of magnetars [2] made theoretical physicists consider matter subject to magnetic field both at high temperatures and low densities and low temperatures and high densities. We describe quark matter subject to strong magnetic fields within the SU(3) (E)PNJL model with vector interaction:

$$
\begin{aligned}
\mathcal{L} = \bar{\psi}_f \left[i\gamma_\mu D^\mu - \hat{m}_f \right] \psi_f \;+\; \mathcal{L}_{sym} \;+\; \mathcal{L}_{det} \\
+ \; \mathcal{L}_{vec} + \mathcal{U}\left(\Phi, \bar{\Phi}; T\right) - \frac{1}{4} F_{\mu\nu} F^{\mu\nu},
\end{aligned}
\tag{1}
$$

with

$$
\mathcal{L}_{sym} = G \sum_{a=0}^{8} \left[(\bar{\psi}_f \lambda_a \psi_f)^2 + (\bar{\psi}_f i\gamma_5 \lambda_a \psi_f)^2 \right],
$$

$$
\mathcal{L}_{det} = -K \left\{ \det_f \left[\bar{\psi}_f (1 + \gamma_5) \psi_f \right] + \det_f \left[\bar{\psi}_f (1 - \gamma_5) \psi_f \right] \right\},
$$

where $\psi_f = (u, d, s)^T$ represents a quark field with three flavors,

$$
\hat{m}_c = \text{diag}_f(m_u, m_d, m_s)
$$

is the corresponding (current) mass matrix, $\lambda_0 = \sqrt{2/3}\,I$ where I is the unit matrix in the three flavor space, and $0 < \lambda_a \leq 8$ denote the Gell-Mann matrices. The

coupling between the magnetic field B and quarks, and between the effective gluon field and quarks is implemented *via* the covariant derivative $D^\mu = \partial^\mu - iq_f A^{EM}_\mu - iA^\mu$ where q_f represents the quark electric charge, $A^{EM}_\mu = \delta_{\mu 2} x_1 B$ is a static and constant magnetic field in the z direction and $F_{\mu\nu} = \partial_\mu A^{EM}_\nu - \partial_\nu A^{EM}_\mu$. To describe the pure gauge sector an effective potential $\mathcal{U}\left(\Phi, \bar{\Phi}; T\right)$ is chosen:

$$\frac{\mathcal{U}\left(\Phi, \bar{\Phi}; T\right)}{T^4} = -\frac{a\left(T\right)}{2} \bar{\Phi}\Phi + b(T) \ln\left[1 - 6\bar{\Phi}\Phi + 4(\bar{\Phi}^3 + \Phi^3) - 3(\bar{\Phi}\Phi)^2\right],$$

where $a\left(T\right) = a_0 + a_1 \left(\frac{T_0}{T}\right) + a_2 \left(\frac{T_0}{T}\right)^2$, $b(T) = b_3 \left(\frac{T_0}{T}\right)^3$. The standard choice of the parameters for the effective potential $\mathcal{U}$ is $a_0 = 3.51$, $a_1 = -2.47$, $a_2 = 15.2$, and $b_3 = -1.75$. Besides the PNJL model, where G denotes the coupling constant of the scalar-type four-quark interaction in the NJL sector, we consider an effective vertex depending on the Polyakov loop $(G(\Phi, \bar{\Phi}))$: the EPNJL model. This effective vertex

$$G(\Phi, \bar{\Phi}) = G\left[1 - \alpha_1 \Phi\bar{\Phi} - \alpha_2(\Phi^3 + \bar{\Phi}^3)\right]. \tag{2}$$

generates entanglement interactions between the Polyakov loop and the chiral condensate.

As for the vector interaction, the Lagrangian density that denotes the $U(3)_V \otimes U(3)_A$ invariant interaction is

$$\mathcal{L}_{vec} = -G_V \sum_{a=0}^{8} \left[(\bar{\psi}\gamma^\mu \lambda_a \psi)^2 + (\bar{\psi}\gamma^\mu \gamma_5 \lambda_a \psi)^2\right]. \tag{3}$$

and a reduced NJLv Lagrangian density can be written as

$$\mathcal{L}_{vec} = -G_V(\bar{\psi}\gamma^\mu \psi)^2. \tag{4}$$

In the SU(3) NJLv model, the above Lagrangian densities are not identical in a mean field approach and we discuss both cases next. We refer to the Lagrangian density given in Eq. (3) as model 1 (P1) and to the Lagrangian density given in Eq. (4) as model 2 (P2).

Our first task was to analyse the possible different phase diagram structures at zero temperature. We have seen that the number of intermediate phases depends on the number of *jumps* appearing in the dressed quark masses, which in turn, depend on the number of filled Landau levels. The chiral susceptibilities, as usually defined, are different not only for the s-quark as compared with the two light quarks, but also for the u and d-quarks, yielding non identical crossover lines for the light quark sector. A typical diagram is shown in Figure 1 and details are given in Ref. [3]. Next, the effect of the vector interaction on three flavor magnetized matter was studied for cold matter within two different models usually found in the literature, a flavor dependent (P1) [4] and a flavor independent one (P2) [5]. We have seen that the flavor independent vector interaction predicts a smaller strangeness content and, therefore, harder equations of state. On the other hand, the flavor dependent vector interaction favors larger strangeness content the larger the vector coupling, as can be seen in Figure 2. At low densities
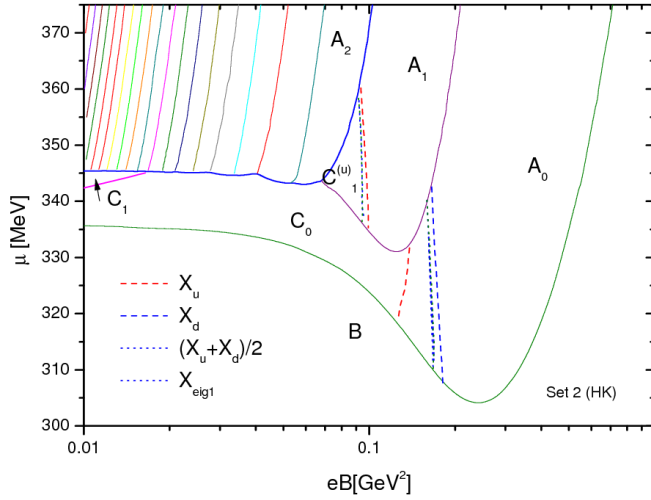
Fig. 1. Phase diagrams in the $eB - \mu$ plane.
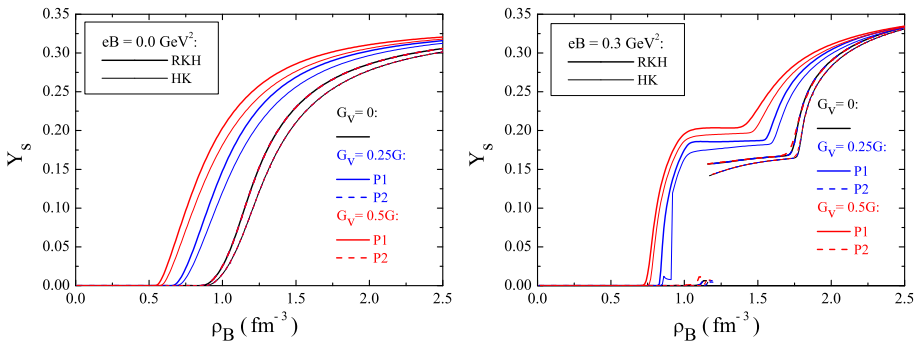
Fig. 2. The strangeness fraction as a function of the baryonic density for models P1 and P2 and different values of G_V, and a) $B = 0$; b) $eB = 0.3\ \text{GeV}^2$.

the magnetic field and the vector interaction have opposite competing effects: the first one softens the equation of state while the second hardens it. Quark stars and hybrid stars subject to an external magnetic field were also studied. Larger star masses are obtained for the flavor independent vector interaction and maximum masses of the order of 2 $M_\odot$ can be achieved depending on the value of the vector interaction and on the intensity of the magnetic field. Hybrid stars may bare a core containing deconfined quarks if neither the vector interaction nor the magnetic field are too strong. Also, the presence of strong magnetic fields seems to disfavor the existence of a quark core in hybrid stars. Mass radius curves for quark and hybrid stars can be seen in Figure 3. Details and quantitative results are given in Ref. [6].

Then, we move to finite temperature and study the behavior of the quark condensates at zero chemical potential within three flavor PNJL and EPNJL models. We have shown that the chiral and deconfinement transition temperatures
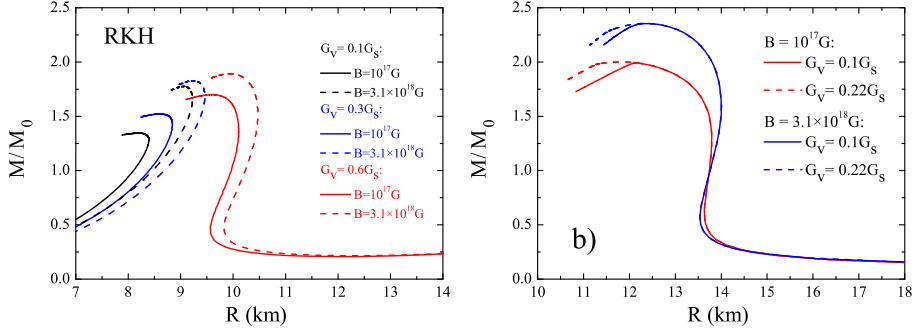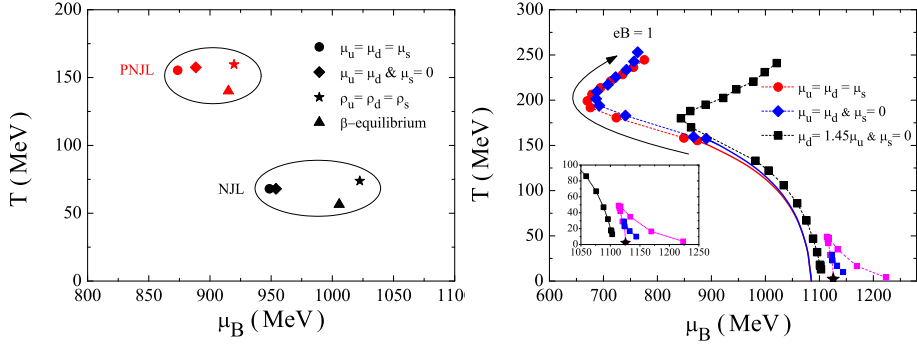
Fig. 3. Mass radius curves obtained with P2 for different values of G_V, two intensities of the magnetic field, parametrization RKH for a) quark and b) hybrid stars.

increase in the presence of an external magnetic field and that, at $T = 0$ the quantitative behaviors of SU(3) PNJL and EPNJL are closer to the lattice results. The effect of the magnetic field on the EPNJL deconfinement and chiral transition temperatures is such that the existing coincidence at $eB = 0$ is destroyed by the magnetic field. For finite temperatures, the inverse magnetic catalysis found in lattice calculations can be obtained if the the magnetic field back-reaction on the Polyakov loop is taken into account by a magnetic field dependent scale parameter T_0. Details about these results are given in Ref. [7].

Finally, the location of the critical end point (CEP) on the QCD phase diagram was calculated within different scenarios with respect to the isospin and strangeness content of matter, as shown in Figure 4 left for non-magnetized matter. It was shown that for β-equilibrium matter the CEP occurs at smaller temperatures and densities. This scenario is of interest for neutron stars and confirms previous calculations that indicate that a deconfinement phase transition in the laboratory will be more easily attained with asymmetric nuclear matter. A more interesting situation was observed when analyzing very isospin asymmetric matter subject to different intensities of the magnetic field, as seen in Figure 4 right. Starting from a scenario having an isospin asymmetry above which the CEP does not exist for a zero external magnetic field it was shown that a sufficiently high external magnetic field could drive the system to a first order phase transition. The critical end point occurs at very small temperatures if $eB < 0.1$ GeV^2 and, in this case, a complicated structure with several CEP at different values of (T, μ_B) are possible for the same magnetic field, because the temperature is not high enough to wash out the Landau level effects. For $eB > 0.1$ GeV^2 only one CEP exists. This is an important result because it shows that a strong magnetic field is able to drive a system with no CEP into a first order phase transition. More details are given in Ref. [8].

Fig. 4. Left - Location of the CEP on a diagram T vs the baryonic chemical potential under different scenarios and models (NJL, PNJL). No external magnetic field is considered. Right - Effect of an external magnetic field on the CEP location within PNJL model for three different scenarios.

References

1. K. Fukushima, D. E. Kharzeev and H. J. Warringa, Phys. Rev. D **78** (2008) 074033; D. E. Kharzeev and H. J. Warringa, Phys. Rev. D **80** (2009) 034028.
2. R. Duncan and C. Thompson, Astrophysical Journal, Part 2 – Letters **392** (1992) L9–L13; C. Kouveliotou et al, Nature **393** (1998) 235.
3. Ana G. Grunfeld, Debora P. Menezes, Marcus B. Pinto and Norberto Scoccola, Phys. Rev. D (2014) in press, arXiv:1402.4731v1 [hep-ph].
4. S. Klimt, M. Lutz, and W. Weise, Phys. Lett. B **249** (1990) 386; M. Hanauske, L. M. Satarov, I. N. Mishustin, H. Stöcker and W. Greiner, Phys. Rev. D **64** (2001) 043005.
5. K. Fukushima, Phys. Rev. D **78** (2008) 114019.
6. Debora P. Menezes, Marcus B. Pinto, Luis R. B de Castro, Constança Providencia and Pedro Costa, Phys. Rev. C **89** (2014) 055207.
7. M. Ferreira, P. Costa, D.P. Menezes, C. Providencia and N. Scoccola, Phys. Rev. D **89** (2014) 016002.
8. Pedro Costa, Márcio Ferreira, Hubert Hansen, Débora P. Menezes, Constança Providência, Phys. Rev. D **89** (2014) 056013.

Schwinger-Dyson approach to QCD explains the genesis of constituent quark masses[⋆]

D. Klabučar[a], D. Kekez[b]

[a] Physics Department, Faculty of Science, Zagreb University, Bijenička c. 32,
10000 Zagreb, Croatia
[b] Rugjer Bošković Institute, Bijenička c. 54, 10000 Zagreb, Croatia

Abstract. Among other successes, the Schwinger-Dyson approach to nonperturbative QCD provides the explanation of the constituent quark model with its quark masses which are very different from the current, Lagrangian masses. Nevertheless, if the interaction kernel contains also the perturbative part of the QCD interaction, the Schwinger-Dyson approach also reproduces the known high-energy behavior of the quark masses predicted by perturbative QCD.

The Schwinger-Dyson (SD) approach to physics of quarks, gluons and hadrons (reviewed, e.g., in Refs. [1–3]) enables the direct contact with their fundamental theory – QCD, through *ab initio* calculations of QCD Green's functions. Also, SD approach permits many phenomenological applications through various degrees of modeling and approximations, which can nevertheless preserve some crucial features of QCD like its chiral behavior.

   In these proceedings we recapitulate from Ref. [4] the part pertaining to the behavior of dressed quark masses, to point out that already several decades ago, the SD approach even at a fairly simple model level provided the correct understanding of the quark masses even in the regime of nonperturbative QCD, and the correct transition between nonperturbative and perturbative regimes of QCD. That is, we explain how SD approach generates dynamically constituent quark masses and thus leads to the constituent quark model in the low energy regime, but is, at the same time, equivalent to the perturbative QCD in the high energy regime if the interaction kernel contains the perturbative QCD part.

   Because of nonperturbative features of QCD at low energies, one must consider the strongly dressed two-point quark Green's function, namely the quark propagator $S(q)$:

$$S^{-1}(q) = A(q^2)\slashed{q} - B(q^2) \, , \tag{1}$$

is dressed very strongly indeed at low quark energies and momenta q. This means that the propagator "vector function" (i.e., wavefunction renormalization) $A(q^2)$ can noticeably depart from 1, and that (what is much more important qualitatively and quantitatively) the propagator "scalar function" $B(q^2)$ can exceed (at

---

[⋆] Talk delivered by D. Klabučar

low q) the light current masses of the lightest (u and d) quarks drastically, by two orders of magnitude. This is the nonperturbative QCD phenomenon of Dynamical Chiral Symmetry Breaking (DχSB), which leads to the momentum-dependent quark mass function $\mathcal{M}(q^2) = B(q^2)/A(q^2)$ with values, at low q^2, of the order of constituent quark masses.

The dressed propagator (1) is obtained by solving the quark two-point ("gap") SD equation for the appropriate quark flavor. But the big trouble with SD equations is that they are a *coupled system* of integral equations for Green's functions of QCD, where an equation for a n-point function "calls" not only other n-point functions (and lower), but also $n+1$-point functions, leading to the intractable growing tower of SD equations, which must be at some point truncated even in *ab initio* SD calculations. Concretely, the "gap" SD equation for the quark propagator $S(q)$ contains *i)* the dressed gluon propagator $\mathcal{G}_{\mu\nu}(q-k)$ and *ii)* the dressed quark-gluon vertex $\Gamma_\nu(k, q-k, q)$, and they both satisfy their own SD equations. However, such SD calculations in the "*ab initio* research direction" are beyond our present scope. Namely, the crucial insight on the dressed quark masses can anyway be obtained by using an "educated Ansatz" $G_{\mu\nu}(q-k)$ instead of a proper solution $\mathcal{G}_{\mu\nu}(q-k)$ for the the dressed gluon propagator, and by resorting to the commonly used rainbow-ladder approximation (*i.e.*, with bare quark-gluon vertices, $\Gamma_\nu(k, q-k, q) \to \gamma_\nu$):

$$S^{-1}(q) = \not{q} - \widetilde{m} - i\, g_{st}^2\, C_F \int \frac{d^4k}{(2\pi)^4} \gamma^\mu S(k) \gamma^\nu G_{\mu\nu}(q-k)\,, \qquad (2)$$

where $\widetilde{m}$ is the bare mass term of the pertinent quark flavor, breaking the chiral symmetry explicitly. For the gluon propagator we use one of those which not only lead to DχSB, but which also provides a remarkably successful description of meson quark-antiquark bound states by the consistent usage in the rainbow-ladder Bethe-Salpeter equation. That is, we use the effective, modeled Landau-gauge gluon propagator of Jain and Munczek [5–7]:

$$g_{st}^2\, C_F G^{\mu\nu}(k) = G(-k^2)(g^{\mu\nu} - \frac{k^\mu k^\nu}{k^2})\,, \qquad (3)$$

where we have indicated that our convention is such that not only the strong coupling constant g_{st}, but also C_F, the second Casimir invariant of the quark representation, are absorbed into the function G. For the present case of $SU(3)_c$, where the group generators are $\lambda^a/2$, namely the (halved) Gell-Mann matrices, $C_F = \frac{4}{3}$.

It is essential that the effective propagator function G is the sum of the perturbative ("ultraviolet") contribution G_{UV} and the nonperturbative ("infrared") contribution G_{IR}:

$$G(Q^2) = G_{UV}(Q^2) + G_{IR}(Q^2)\,, \quad (Q^2 = -k^2)\,. \qquad (4)$$

The perturbative part G_{UV} is required to reproduce correctly the ultraviolet (UV) asymptotic behavior that unambiguously follows from QCD in its high–energy, perturbative regime. Therefore, this part must essentially be given – up to the factor $1/Q^2$ – by the running coupling constant $\alpha_{st}(Q^2)$ which is well-known from perturbative QCD, so that G_{UV} is in fact *not* modeled.
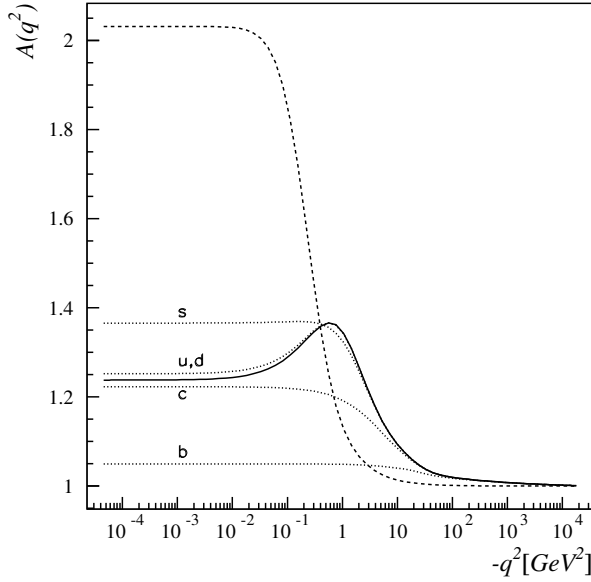
Fig. 1. Our chiral-limit solution (the solid line) for the propagator function $A(q^2)$ is compared with our massive solutions for various $\tilde{m}(\Lambda) \neq 0$ (the dotted lines marked by letters denoting the pertinent flavors). The dashed line denotes the $A(q^2)$-*Ansatz* (for u, d-quarks) of [8], and also of Frank *et al.* [9] who have such parameters that the difference with respect to the dashed line [8] cannot be seen on this figure.

From the renormalization group, in the spacelike region ($Q^2 = -k^2$),

$$
G_{UV}(Q^2) = 4\pi C_F \frac{\alpha_{st}(Q^2)}{Q^2} \approx \frac{4\pi^2 C_F d}{Q^2 \ln(x_0 + \frac{Q^2}{\Lambda_{QCD}^2})} \left\{ 1 + b \frac{\ln[\ln(x_0 + \frac{Q^2}{\Lambda_{QCD}^2})]}{\ln(x_0 + \frac{Q^2}{\Lambda_{QCD}^2})} \right\},
$$
(5)

where we employ the two–loop asymptotic expression for $\alpha_{st}(Q^2)$, and where $d = 12/(33 - 2N_f)$, $b = 2\beta_2/\beta_1^2 = 2(19N_f/12 - 51/4)/(N_f/3 - 11/2)^2$, and N_f is the number of quark flavors. The parameter x_0 is the infrared cutoff, introduced to regulate the logarithmic behavior of G_{UV} as the values of Q^2 approach Λ_{QCD}^2, the dimensional parameter of QCD. As in [7], we use $x_0 = 10$, but this is not really important since the results are only very weakly sensitive to the values of x_0, as was already pointed out by [7]. Following [7], we set $N_f = 5$ and $\Lambda_{QCD} = 228$ MeV. Although the top quark has meanwhile been found, its mass scale is far above the range of momenta relevant for nonperturbative and bound state calculations, and even above the value of the UV cutoff needed in the massive version of our SD equations (see below). Therefore, there is no need to revise G_{UV} (5) to include $N_f = 6$. (On the other hand, choosing N_f below 5 would not be satisfactory because *(i)* the momentum range of the order of the b quark mass still has non-negligible influence in our bound-state calculations, *(ii)* the b quark mass is below the UV cutoff used in our "massive SD equations", and *(iii)*

sometimes we need the solutions for relatively high momenta, *e.g.*, to be able to see the asymptotic behavior of the propagator functions $A(q^2)$ and $B(q^2)$ – see Figs. 1, 2 and 3.)

The case $\widetilde{m} = 0$ corresponds to the chiral limit where the current quark mass $m = 0$, and where DχSB is the one and only cause ("source") of the constituent quark mass, defined as the mass function value at $q^2 = 0$, namely $\mathcal{M}(0) = B(0)/A(0)$ [5]. Of course, calling "the constituent mass" the value of the "momentum-dependent constituent mass function" $B(q^2)/A(q^2)$ at exactly $q^2 = 0$ and not on some other low q^2, is a matter of a somewhat arbitrary choice. Another conventional choice (*e.g.*, in [10]) is to call the solution of $-q^2 = B^2(q^2)/A^2(q^2)$ the Euclidean constituent-quark mass squared. However, since this is just a matter of choosing terminology, we stick to that of Jain and Munczek [6].

With the assumption that u and d quarks are massless, which is an excellent approximation in the context of hadronic physics, solving of (2) yields the solutions for $A(q^2)$ and $B(q^2)$, displayed in respective Fig. 1 and Fig. 2 by the solid lines.

In these figures we also compare them with $A(q^2)$ and $B(q^2)$ corresponding to the dressed propagator *Ansätze* of the references [8,9], represented by the dashed lines. Our massless solutions lead to the constituent u (and d) quark mass $B(0)/A(0) = 356$ MeV. The ratio $B(q^2)/A(q^2)$, namely our momentum-dependent mass function $\mathcal{M}(q^2)$, is depicted in Fig. 3 by the solid line, and the dashed line represents the analogous ratio formed from $A(q^2)$ and $B(q^2)$ corresponding to the *Ansätze* of Refs. [8,9].

Note that our chiral-limit solutions for $A(q^2)$ and $B(q^2)$ differ a lot from the *Ansätze* of Refs. [8,9], even though the ratio, giving the mass function, is similar.

When $\widetilde{m} \neq 0$, the SD equation (2) must be regularized by a UV cutoff Λ [6,7], and the bare mass $\widetilde{m}$ is in fact a cutoff–dependent quantity. We adopted the parameters of [7], where (for $\Lambda = 134$ GeV) $\widetilde{m}(\Lambda^2)$ is 3.1 MeV for the isosymmetric u- and d-quarks, 73 MeV for s–quarks, 680 MeV for c–quarks, and 3.3 GeV for b–quarks. Solving of (2) then yields the solutions $A(q^2)$ and $B(q^2)$ for "slightly massive" u- and d-quarks, "intermediately massive" s-quarks, as well as the solutions for the heavy quarks c and b. We essentially reproduce the results of Ref. [7] (within the accuracy permitted by numerical uncertainties). The $A(q^2)$ and $B(q^2)$ solutions for $\widetilde{m}(\Lambda^2) \neq 0$ are displayed in Figs. 1 and 2 by dotted lines marked by u, d and s, c and b, indicating which flavor a curve pertains to. For the lightest, u- and d-quarks (with $\widetilde{m} = 3.1$ MeV), both $A(q^2)$ and $B(q^2)$ are only slightly above the curves representing our respective chiral-limit solutions. More precisely, the difference is then at most 1.4% (at $q^2 = 0$) for $A(q^2)$, while for $B(q^2)$ the largest absolute value of the difference (again occurring at $q^2 = 0$) amounts to an excess of 6.2% over our chiral-limit solution. The excess quickly becomes much smaller above $-q^2 = 0.2$ GeV. Admittedly, at $-q^2$ above 2 GeV, the *relative* difference between the "chiral" and "slightly massive" $B(q^2)$'s starts growing again because of the different asymptotic behaviors of these respective solutions. They are, respectively, $B(q^2) \sim [\ln(-q^2/\Lambda_{\text{QCD}}^2)]^{d-1}/q^2$ and $B(q^2) \sim 1/[\ln(-q^2/\Lambda_{\text{QCD}}^2)]^d$, and are consistent with the asymptotic freedom of QCD [11, 12]. (This in turn results in the asymptotic behavior of the momentum-
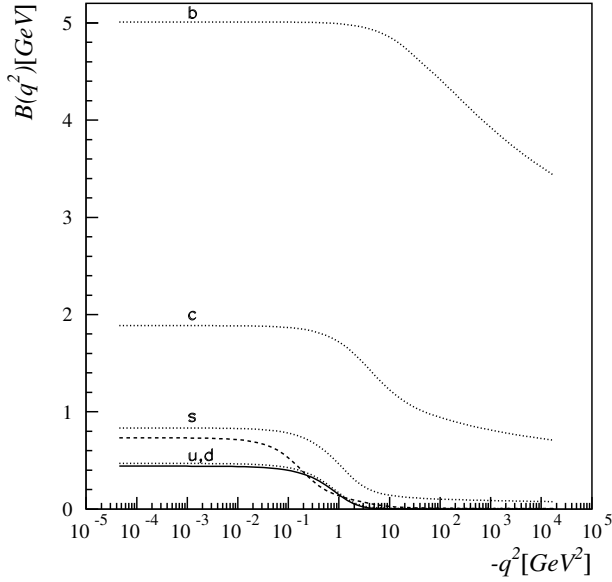
Fig. 2. The comparison of our chiral-limit solution (the solid line) for the propagator function $B(q^2)$ with our massive solutions for various $\widetilde{m}(\Lambda) \neq 0$ represented by the dotted lines marked by letters denoting the pertinent flavors, and with the *Ansatz* (for u, d-quarks) for $B(q^2)$ employed by [8] (the dashed line), and that of [9], which cannot be distinguished from the dashed line in this plot.

dependent, dynamical mass functions $B(q^2)/A(q^2)$, which is in accord with the behavior in perturbative QCD [5–7,12,13]). However, the absolute values of these $B(q^2)$'s (even for the "slightly massive" case) and of their difference are already very small at $-q^2 > 2$ GeV.

The deep Euclidean asymptotic behavior $B(q^2) \sim 1/[\ln(-q^2/\Lambda^2_{QCD})]^d$ is fulfilled also for the more massive flavors, but of course with very different coefficients (which are essentially proportional to the current quark masses [6, 7]). Also, $A(q^2) \to 1$ for all flavors as $-q^2 \to \infty$. For low $-q^2$, however, $A(q^2)$'s belonging to different flavors exhibit interesting differences. The bump that characterizes the least massive (or chiral) u, d-quarks is absent already in $A(q^2)$ of our "intermediately massive" s-quark, for which the fall-off is almost monotonical, as the increase (around $-q^2 \sim 0.1$ GeV) above the $A(0)$-value is practically imperceptibly small. Moreover, for even heavier c— and especially b—quarks, the $A(q^2)$-values for even lowest $-q^2$'s, are below the corresponding values of the chiral-limit $A(q^2)$. Comparing the various $A(q^2)$- and $B(q^2)$-solutions illustrates well how the importance of the dynamical dressing decreases as one considers increasingly massive quark flavors.

These $\widetilde{m} \neq 0$ solutions give us the constituent mass $B(0)/A(0)$ of 375 MeV for the (isosymmetric) u- and d-quarks, 610 MeV for the s-quarks, 1.54 GeV for the c–quarks, and 4.77 GeV for the b–quarks. These are very reasonable values. Also,
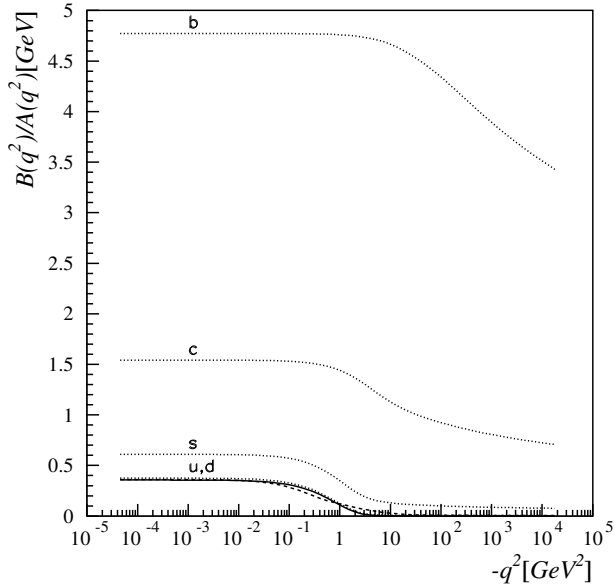
Fig. 3. The solid line denotes our constituent quark mass function $B(q^2)/A(q^2)$ in the chiral limit, while the dotted lines (marked by letters indicating the pertinent flavors) denote our constituent quark mass functions for $\widetilde{m}(\Lambda) \neq 0$. The one following from the *Ansätze* of [8,9] is denoted by the dashed line.

the momentum-dependent mass functions $B(q^2)/A(q^2)$ – depicted in Fig. 3 – in the presently chosen variant of the SD approach [5–7] behave for all flavors in the way which correctly captures the differences between heavy and light quarks and qualitatively agrees with the most advanced recent results on the quark masses in the SD approach such as Ref. [14], where instead of simple regularization [6,7] the full nonperturbative renormalization has been carried out and the quantitative agreement with quenched lattice results achieved over a very wide range of momenta.

References

1. C. D. Roberts and A. G. Williams, *Prog. Part. Nucl. Phys.* **33**, 477 (1994).
2. R. Alkofer and L. von Smekal, *Phys. Rept.* **353**, 281 (2001) [hep-ph/0007355].
3. I. C. Cloet and C. D. Roberts, *Prog. Part. Nucl. Phys.* **77**, 1 (2014) [arXiv:1310.2651 [nucl-th]].
4. D. Kekez, B. Bistrovic and D. Klabucar, Int. J. Mod. Phys. A **14**, 161 (1999) [hep-ph/9809245].

5. P. Jain and H. J. Munczek, *Phys. Rev.* **D44**, 1873 (1991).

6. H. J. Munczek and P. Jain, *Phys. Rev.* **D46**, 438 (1992).

7. P. Jain and H. J. Munczek, *Phys. Rev.* **D48**, 5403 (1993).

8. C. D. Roberts, *Nucl. Phys.* **A605**, 475 (1996)
   C. D. Roberts, in: *Chiral Dynamics: Theory and Experiment*, eds. A. M. Bernstein and B. R. Holstein, *Lecture Notes in Physics, Vol.* **452** (Springer, Berlin, 1995) p. 68.

9. M. R. Frank, K. L. Mitchell, C. D. Roberts and P. C. Tandy, *Phys. Lett.* **B359**, 17 (1995).

10. P. Maris and C. D. Roberts, *Phys. Rev.* **C56**, 3369 (1997).

11. K. Lane, *Phys. Rev.* **D10**, 2605 (1974).

12. H. D. Politzer, *Nucl. Phys.* **B117**, 397 (1976).

13. R. Tarrach, *Nucl. Phys.* **B183**, 384 (1981).

14. M. S. Bhagwat, M. A. Pichowsky, C. D. Roberts and P. C. Tandy, Phys. Rev. C **68**, 015203 (2003) [nucl-th/0304003].

Mesonic Effects in Baryon Ground and Resonant States[*]

R. Kleinhappel[a], L. Canton[b], W. Plessas[a], and W. Schweiger[a]

[a] Theoretical Physics, Institute of Physics, University of Graz, Universitätsplatz 5, A-8010 Graz, Austria
[b] Istituto Nazionale di Fisica Nucleare, Via F. Marzolo 8, I-35131 Padova, Italy

Abstract. We investigate mesonic effects in baryon ground and resonant states by including meson loops in a relativistic coupled-channels approach. From calculations, so far done on the hadronic level, we obtain results for the dressed mass of the nucleon ground state and for dressed masses and decay widths of resonances, notably of the Δ, due to coupling to the pion channel. At this stage an improvement is found over the single-channel theory, the experimental data for decay widths, however, are still underestimated.

A proper description of hadron resonances still represents a big challenge in quantum chromodynamics (QCD), irrespective of the approach followed. Particularly in the framework of constituent-quark models, hadronic resonances are usually treated as excited bound states rather than as resonant states with finite widths. Calculations of strong decays have thus shown short-comings generally producing too small decay widths [1–4]. To remedy this situation we are investigating a coupled-channels (CC) approach taking into account explicit meson, especially pionic, degrees of freedom.

The CC approach has been tested before within a simple scalar toy model, leaving out all spin and flavor dependences. It turned out that the coupling to a mesonic channel shifts the ground-state mass down and generates the resonant state with a finite width, whose magnitude is dependent essentially on the coupling strength to the meson channel [5,6]. Recently we have obtained results for the πNN and the $\pi N\Delta$ systems, including all spin and flavor degrees of freedom.

Our theory relies on a relativistically invariant mass operator written in matrix form. It contains a bare baryon state i, here the N or Δ, coupled to the πNN and the $\pi N\Delta$ channels $i + 1$, respectively. After eliminating the latter by the Feshbach method one ends up with the following eigenvalue problem for the dressed baryon ground or resonant state $|\psi_i >$:

$$\left[M_i - K \left(m - M_{i+1} + i0 \right)^{-1} K^\dagger \right] |\psi_i >= m|\psi_i > \ . \tag{1}$$

Evidently, it contains an optical potential, which becomes complex above the πN threshold. Herein, M_i and M_{i+1} are the invariant mass operators of the i-th and

---

[*] Talk presented by R. Kleinhappel

(i+1)-st channels and K describes the transition dynamics. It should be noted that the mass eigenvalue m appears also in the optical-potential term. Beyond the resonance threshold it acquires an imaginary part leading to a finite decay widths.

The transition dynamics contained in K is deduced from the following Lagrangian densities

$$\mathcal{L}_{NN\pi} = -\frac{f_{NN\pi}}{m_\pi}\bar{\Psi}\gamma_5\gamma^\mu\Psi\partial_\mu\Phi\,, \tag{2}$$

$$\mathcal{L}_{\Delta N\pi} = -\frac{f_{\Delta N\pi}}{m_\pi}\bar{\Psi}\Psi^\mu\partial_\mu\Phi + h.c.. \tag{3}$$

where Ψ and Ψ^μ represent the N and Δ fields, which are coupled in pseudovector form by the π field Φ with strengths $f_{NN\pi}$ and $f_{\Delta N\pi}$, respectively. This leads to transition matrix elements from the bare $\tilde{N}$ and $\tilde{\Delta}$ states to the channels including the explicit pions (with mass m_π) for the cases of πNN

$$< \tilde{N}|\mathcal{L}_{\pi\tilde{N}\tilde{N}}(0)|\tilde{N},\pi;k''_\pi >= \sum \frac{i\,f_{\pi\tilde{N}\tilde{N}}}{m_\pi}\bar{u}(k_{\tilde{N}},\Sigma_{\tilde{N}})\gamma^\mu\gamma_5 u(k''_{\tilde{N}},\Sigma''_{\tilde{N}})(k''_\pi)_\mu \tag{4}$$

and $\pi N\Delta$

$$< \tilde{\Delta}|\mathcal{L}_{\pi\tilde{N}\tilde{\Delta}}(0)|\tilde{N},\pi;k''_\pi >= \sum \frac{i\,f_{\pi\tilde{N}\tilde{\Delta}}}{m_\pi}\bar{u}^\mu(k_{\tilde{\Delta}},\Sigma_{\tilde{\Delta}})u(k''_{\tilde{N}},\Sigma''_{\tilde{N}})(k''_\pi)_\mu\,. \tag{5}$$

Here $u\,(k_N,\Sigma_N)$ are the spin-$\frac{1}{2}$ Dirac spinors of the N and $u^\mu\,(k_\Delta,\Sigma_\Delta)$ the spin-$\frac{3}{2}$ Rarita-Schwinger spinors of the Δ. In the rest frame of the baryon B the eigenvalue equation (1) finally turns into the following explicit form

$$\left(m_{\tilde{B}} + \int \frac{d^3k''_\pi}{(2\pi)^3}\frac{1}{2\omega''_\pi 2\omega''_{\tilde{N}}2m_{\tilde{B}}}\mathcal{F}_{\pi\tilde{N}\tilde{B}}(k''_\pi) < \tilde{B}|\mathcal{L}_{\pi\tilde{N}\tilde{B}}(0)|\tilde{N},\pi;k''_\pi >\right.$$
$$\times \left(m - \sqrt{m_{\tilde{N}}^2 + k''^2_\pi} - \sqrt{m_\pi^2 + k''^2_\pi} + i0\right)^{-1}\mathcal{F}^*_{\pi\tilde{N}\tilde{B}}(k''_\pi)$$
$$\left.\times < \tilde{N},\pi;k''_\pi|\mathcal{L}^\dagger_{\pi\tilde{N}\tilde{N}}(0)|\tilde{B} >\right) < \tilde{B}|\psi_B >= m < \tilde{B}|\psi_B > \tag{6}$$

with B standing for N or Δ and all quantities with a tilde referring to bare particles. The wave functions of the baryon states $< \tilde{B}|\psi_B >$ are represented by free momentum eigenstates denoted by $< \tilde{B}|$ or equivalently by free velocity states $< \tilde{B};v = 0|$ (for pertinent details see Ref. [5]). The processes corresponding to the optical potential in Eq. (6) are depicted in Fig. 1.
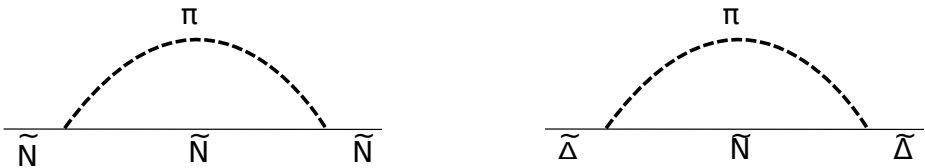

Fig. 1. Pion-loop diagrams for the πNN and $\pi N\Delta$ systems according to Eq. (6).

In Eq. (6) we have inserted form factors $\mathcal{F}_{\pi\tilde{N}\tilde{B}}$ for the extended meson-baryon vertices. They are taken from three different models, namely, a relativistic constituent-quark model (RCQM) [7,8] as well as two phenomenological meson-nucleon models, namely, the one by Sato and Lee (SL) [9] and the one by Polinder and Rijken (PR) [10]. The corresponding parametrizations are all given in Ref. [11] according to the form

$$F\left(\mathbf{q}^2\right) = \frac{1}{1 + \left(\frac{q}{\Lambda_1}\right)^2 + \left(\frac{q}{\Lambda_2}\right)^4} . \tag{7}$$

The cut-off parameters occurring in Eq. (7) and the values of the coupling constants are summarized in Tab. 1. The functional dependences of the various vertex form factors are shown in Figs. 2 and 3.

|		RCQM	SL	PR
N	$\frac{f_N^2}{4\pi}$	0.0691	0.08	0.013
	Λ_1	0.451	0.453	0.940
	Λ_2	0.931	0.641	1.102
Δ	$\frac{f_\Delta^2}{4\pi}$	0.188	0.334	0.167
	Λ_1	0.594	0.458	0.853
	Λ_2	0.998	0.648	1.014

Table 1. πNN and πNΔ coupling constants as well as cut-off parameters entering into Eq. (7) for the three different form-factor models used in the present work (cf. Ref. [11]).

By solving the eigenvalue equation (6) with the physical nucleon mass $m_N = 939$ MeV as input for m we find the bare nucleon mass $m_{\tilde{N}}$ and thus the influence of the pion loop. Tab. 2 contains the results for the pion dressing of the nucleon ground state. It is seen that all three different form-factor models lead to very similar magnitudes for the mass differences $m_N - m_{\tilde{N}}$ of about 100 MeV.

	RCQM	SL	PR
$m_{\tilde{N}}$	1.067	1.031	1.051
$m_N - m_{\tilde{N}}$	-0.128	-0.092	-0.112

Table 2. Mesonic effects on the nucleon mass m_N from coupling to the πNN channel.

In the case of the Δ resonance we are interested in the mesonic effects on both the mass as well as the decay width. In the first instance, we employ a bare intermediate nucleon $\tilde{N}$ as is shown in the graph on the r.h.s. of Fig. 1. The corresponding results are given in Tab. 3. Again the pionic effects on the masses are quite similar for the three different form-factor models. The π-decay widths,
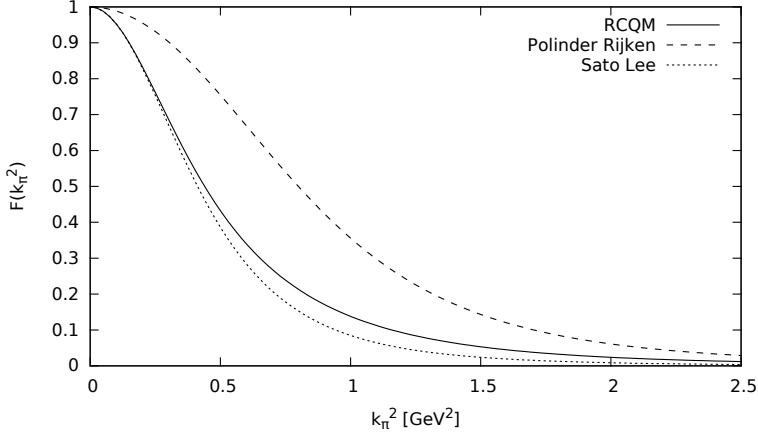
Fig. 2. Momentum dependences of the three different form-factor models in case of the πNN system.
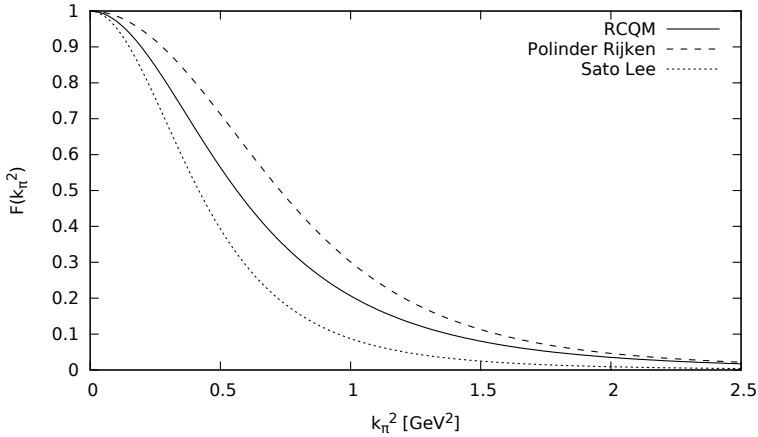
Fig. 3. Momentum dependences of the three different form-factor models in case of the $\pi N \Delta$ system.

however, show bigger variations. Still, they are all too small as compared to the phenomenological value.

A more realistic description of the $\Delta \rightarrow N\pi$ decay width is obtained by replacing the bare $\tilde{N}$ with mass $m_{\tilde{N}}$ in the intermediate state by the physical nucleon N with mass $m_N = 939$ MeV, as depicted in Fig. 4.

The corresponding results are given in Tab. 4. It is immediately seen that the decay widths get much enhanced, while the effects on the masses are only slightly changed. We expect the larger phase space for the pionic decay to be responsible for the enhancement of the decay widths.

At this stage an open problem is left with regard to dressing the vertex form factors and the coupling strengths in our work. Corresponding studies have ear-

	RCQM	SL	PR
$m_{\tilde{N}}$	1.067	1.031	1.051
$m_{\tilde{\Delta}}$	1.300	1.295	1.336
$\mathrm{Re}\,(m_\Delta) - m_{\tilde{\Delta}}$	-0.068	-0.062	-0.104
$\Gamma = 2\,\mathrm{Im}\,(m_\Delta)$	0.0026	0.017	0.0048

Table 3. Mesonic effects on the Δ mass $\mathrm{Re}\,(m_\Delta)$ and π-decay width Γ from coupling to the $\pi N\Delta$ channel, according to the loop diagram on the r.h.s. of Fig. 1. The bare nucleon masses $m_{\tilde{N}}$ are the same as in Tab. 2.
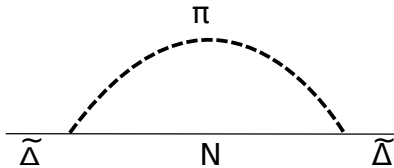
Fig. 4. Pion-loop diagram for the $\pi N\Delta$ system with an intermediate physical nucleon with mass $m_N = 939$ MeV.

	RCQM	SL	PR
m_N	0.939	0.939	0.939
$m_{\tilde{\Delta}}$	1.318	1.306	1.358
$\mathrm{Re}\,(m_\Delta) - m_{\tilde{\Delta}}$	-0.086	-0.073	-0.125
$\Gamma = 2\,\mathrm{Im}\,(m_\Delta)$	0.042	0.069	0.039

Table 4. Mesonic effects on the Δ mass $\mathrm{Re}\,(m_\Delta)$ and π-decay width Γ from coupling to the $\pi N\Delta$ channel, according to the loop diagram in Fig. 4.

lier been undertaken, e.g., by both Sato and Lee [9] as well as Polinder and Rijken [10]. We may expect a further improvement of our results by following a similar way, but it constitutes a difficult task to realize such a framework consistently in our approach.

In summary we are encouraged by the results obtained so far. We have identified the magnitudes of the pionic effects on the N ground state as well as the Δ resonance. In addition, we could demonstrate, how the pionic Δ decay width comes about by explicitly including the π-decay channel. Analogous investigations are presently under way for the N^* resonances.

Acknowledgment

References

1. T. Melde, W. Plessas, and R. F. Wagenbrunn, Phys. Rev. C **72**, 015207 (2005); ibid. C **74**, 069901 (2006).

2. T. Melde, W. Plessas, and B. Sengl, Phys. Rev. C **76**, 025204 (2007).
3. B. Sengl, T. Melde, and W. Plessas, Phys. Rev. D **76**, 054008 (2007).
4. T. Melde, W. Plessas, and B. Sengl, Phys. Rev. D **77**, 114002 (2008).
5. R. Kleinhappel, Diploma Thesis, University of Graz, 2010.
6. R. Kleinhappel and W. Schweiger, in: *Dressing Hadrons* (Proceedings of the Mini-Workshop, Bled, Slovenia, 2010), ed. by B. Golli, M. Rosina, and S. Sirca, DMFA, Ljubljana (2010), p. 33; arXiv:1010.3919.
7. L.Y. Glozman, W. Plessas, K. Varga, and R.F. Wagenbrunn, Phys. Rev. D **58**, 094030 (1998).
8. L.Y. Glozman, Z. Papp, W. Plessas, K. Varga, and R.F. Wagenbrunn, Phys. Rev. C **57**, 3406 (1998) .
9. T. Sato and T. S. H. Lee, Phys. Rev. C **54**, 2660 (1996).
10. H. Polinder and T. A. Rijken, Phys. Rev. C **72**, 065210 (2005); ibid. C **72**, 065211 (2005).
11. T. Melde, L. Canton, and W. Plessas, Phys. Rev. Lett. **102**, 132002 (2009).

Overlap quark propagator in Coulomb-gauge QCD[*]

Y. Delgado[a], M. Pak[a], M. Schröck[b]

[a] Institut für Physik, Karl-Franzenz Universität Graz, 8010 Graz, Austria
[b] Istituto Nazionale di Fisica Nucleare (INFN), Sezione di Roma Tre, Rome, Italy

Abstract. The quark propagator is examined on quenched gauge field configurations in Coulomb Gauge using chirally symmetric Overlap fermions. In this gauge the dressing functions of the quark propagator can be related to the confinement and chiral symmetry properties of QCD. Confinement can be attributed to the infrared divergent vector dressing function. The dressing functions of the quark propagator are evaluated, the dynamical quark mass is extracted and the chiral extrapolation of these quantities is performed. Furthermore, the issue of Dirac low-mode removal is discussed.

1 Introduction

The quark propagator is the central object for computing hadronic correlators, from which baryon and meson masses are extracted. In the continuum approach, it is the central ingredient for the Bethe–Salper equation. The gauge has to be fixed in order to analyze its behavior. We choose Coulomb gauge, where the longitudinal part of the gauge field is eliminated and the so-called color-Coulomb potential arises, which is the QCD analogue of the QED Coulomb potential and which describes the interaction between two static color sources. Continuum methods in Coulomb gauge, especially the variational approach, Ref. [1], have been used mainly to study the pure Yang-Mills part of the theory.

Although progress has been made also in the quark sector in recent years, Refs. [2, 3], the quark propagator in Coulomb gauge is not yet well understood. Lattice studies are highly needed, especially to improve on the still widely used rainbow-ladder Dyson-Schwinger equations. The only lattice study in this direction has been performed in Ref. [4]. We use Overlap fermions for this purpose, which allow for a clear and unambiguous examination of the dressing functions. With non-chiral fermions tree-level corrections and improvement techniques have to be applied. Overlap Dirac propagator studies in Landau gauge can be found in Refs. [5, 6].

Another motivation of this work is to explore a phase, where chiral symmetry is restored by hand in the vacuum. What happens to the confinement properties in such a situation? We argue that we get a clearer picture of this issue by analyzing the dressing functions of the quark propagator.

---

[*] Talk delivered by M. Pak

This contribution is organized as follows: In Chapter 2 the Overlap Dirac operator is introduced and in chapter 3 the lattice setup is discussed. In Chapter 4 the main features of the Coulomb gauge quark propagator and our lattice results are presented. The issue of low-mode removal is shortly discussed. In Chapter 5 a conclusion and an outlook are given.

2   Overlap Dirac operator and free propagator

We use the following parameterization for the massive Overlap Dirac operator, Ref. [7],

$$D(m_0) = \left(1 - \frac{m_0}{2\rho}\right) D(0) + m_0 \,, \tag{1}$$

with

$$D(0) = \rho \left(\mathbb{1} + \gamma_5 \,\text{sign}\,[H_W(-\rho)]\right) \,, \tag{2}$$

where $H_W(-\rho) = \alpha\gamma_5 D_W(-\rho)$ is the Hermitian Wilson-Dirac operator, m_0 the mass parameter and ρ the negative mass of the Wilson-Dirac operator, which is set to the value 1.6 throughout this work. The massless Ovelap-Dirac operator $D(0)$ is an explicit solution of the Ginsparg-Wilson equation and therefore describes exactly massless quarks on the lattice. The eigenvalues lie on a circle in the complex plane with radius ρ. Exact zero modes occur and a lattice version of the index theorem can be defined, see Ref. [8].

To make contact with continuum physics, we impose for the massless Overlap propagator

$$\widetilde{S} = S - \frac{1}{2\rho} \,, \tag{3}$$

from which continuum chiral symmetry follows. The structure of the free (massive) propagator is given as

$$\left(\widetilde{S}^{(0)}\right)^{-1}(p) = i\gamma_\mu q_\mu + \mathbb{1}m \,. \tag{4}$$

The Overlap lattice momentum q_μ and current quark mass m are computed as

$$q_\mu = \frac{4\rho^2}{(2\rho - m_0)} \frac{k_\mu \left(\sqrt{k_\mu^2 + A^2} + A\right)}{k_\mu^2} \,, \quad m = \frac{m_0}{1 - \frac{m_0}{2\rho}} \,, \tag{5}$$

which can be obtained from Eq. (4) and which are used in the extraction of the lattice dressing functions.

3   Lattice setup

Using the Chroma software package [9] and QDP-JIT [10, 11], configurations are generated on a 20^4 lattice at $\beta = 7.552$ ($a = 0.2$ fm) with the Lüscher-Weisz [12]

gauge action. The configurations are then fixed to Coulomb gauge ($\partial_i A_i = 0$). However, the temporal links are not affected by this procedure and are fixed to the Integrated Polyakov loop gauge. For further details, see Ref. [13].

With an ensemble of 96 configurations we evaluate the quark propagator for six current quark masses chosen at $m = (0.085, 0.092, 0.099, 0.113, 0.137, 0.173)$ GeV. The Dirac matrix is inverted on point sources for each configuration. Subsequently, the quark propagators are transformed to momentum space after which the extraction of the dressing functions is performed according to the description given in [4, 14].

4   Non-perturbative quark propagator

In Coulomb gauge the non-perturbative quark propagator is parameterized by four independent dressing functions

$$S^{-1}(\mathbf{p}, p_4) = i\gamma_i p_i A_S(\mathbf{p}) + i\gamma_4 p_4 A_T(\mathbf{p}) + \gamma_4 p_4 \gamma_i p_i A_D(\mathbf{p}) + \mathbb{1} B(\mathbf{p}) \ . \quad (6)$$

Here A_S, A_T, A_D, B are *spatial*, *temporal*, *mixed* and *scalar* dressing functions, respectively. We observe that *all* dressing functions are independent of p_4, which was also observed in Ref. [4]. We note that the temporal part $A_T(\mathbf{p})$ vanishes if the additional gauge freedom with respect to space independent gauge transformations is not fixed. A possible mixed component $A_D(\mathbf{p})$, which does not appear at tree-level, also seems to vanish non-perturbatively, see left-hand side of Fig. 1. The temporal dressing function $A_T(\mathbf{p})$, which does not depend on the Coulomb gauge condition, seems to approach a finite value in the IR, although the error bars are too large to make a precise statement, see right-hand side of Fig. 1.

From mean-field studies in continuum Coulomb gauge it is argued that, due to the presence of the linear confinement potential, the scalar and vector dressing functions diverge as $|\mathbf{p}| \to 0$, see Ref. [15]. However, the dynamical quark mass $M(\mathbf{p}) = B(\mathbf{p})/A_S(\mathbf{p})$ becomes constant for $|\mathbf{p}| \to 0$, identified as the constituent quark mass. This is a remarkable result: the divergencies in the dressing functions have to cancel each other to give a finite infrared mass. Since the lattice imposes an infrared regulator, we do not observe a divergence. However, we observe that both dressing functions $B(\mathbf{p})$ and $A_S(\mathbf{p})$ increase for small momenta, see Fig. 2. It can be seen, that in the chiral limit a non-vanishing scalar dressing function appears. This is a clear signal for chiral symmetry breaking and dynamical mass generation. From the dynamical mass function $M(\mathbf{p})$ in Fig. 3, we observe that around 1 GeV mass generation sets in and that a constituent mass for chiral quarks around 300 MeV is reached.

Finally let us comment on an interesting observation in Coulomb gauge. Since all dressing functions are independent of p_4, the static quark propagator can be evaluated, yielding

$$S(\mathbf{p}) = \frac{B(\mathbf{p}) - i\boldsymbol{\gamma} \cdot \mathbf{p} A_S(\mathbf{p})}{2\omega(\mathbf{p})}, \quad (7)$$
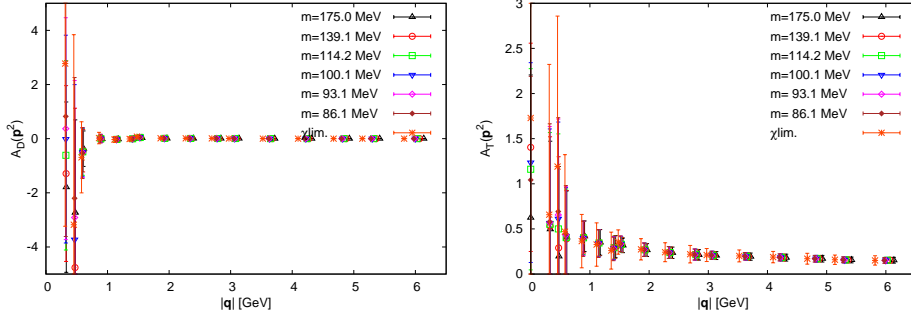
Fig. 1. *Mixed component $A_D(\mathbf{p})$ (l.h.s.) and temporal component $A_T(\mathbf{p})$ (r.h.s.) for several current quark masses m and in the chiral limit.*

and the quark dispersion relation $\omega(\mathbf{p})$ is identified as

$$\omega(\mathbf{p}) = A_T(\mathbf{p})A_S(\mathbf{p})\sqrt{\mathbf{p}^2 + M^2(\mathbf{p})} \, . \tag{8}$$

Since the vector dressing functions $A_S(\mathbf{p})$ is a divergent quantity in the infrared, the energy dispersion $\omega(\mathbf{p})$ is divergent as well. This issue has a clear physical implication: the excitation energy of a confined quark is infinite. Such a mechanism of quark confinement makes Coulomb gauge appealing.

Now a question arises: if one removes the chiral condensate from the quark propagator, is the energy dispersion $\omega(\mathbf{p})$ still infrared divergent? If yes, then confinement is intact, although chiral symmetry has been artificially restored in the vacuum. We expect that, after chiral symmetry restoration, the quark condensate $\langle\bar{\psi}\psi\rangle$ and therefore the dynamical quark mass $M(\mathbf{p})$ as well as the scalar dressing function $B(\mathbf{p})$ vanish in the chiral limit. However, the interesting question will be, how the vector dressing function $A_S(\mathbf{p})$ is affected by artificial chiral symmetry restoration. First results show that the spatial dressing function does not change its shape. This suggests that $A_S(\mathbf{p})$ is still infrared divergent in the continuum limit. A single quark is still removed from the spectrum. This conclusion supports recent hadron spectroscopy studies, see Refs. [16, 17]. Our final results on this issue will be presented elsewhere, Ref. [18].

5   Summary and conclusions

First steps in a detailed analysis of the Overlap quark propagator in Coulomb gauge have been presented. A clear indication of dynamical mass generation is observed and a constituent mass around 300 MeV is obtained. Scalar and vector dressing functions increase for small momenta. If a divergent behavior is present has to be left to a future work. Moreover, it is shown that in Coulomb gauge confinement and chiral symmetry breaking can be linked to each other by a quark dispersion relation. It is shown that via the vector dressing function it can be judged if confinement is still intact when chiral symmetry is artificially restored by removing the low-lying Dirac eigenmodes from the spectrum.
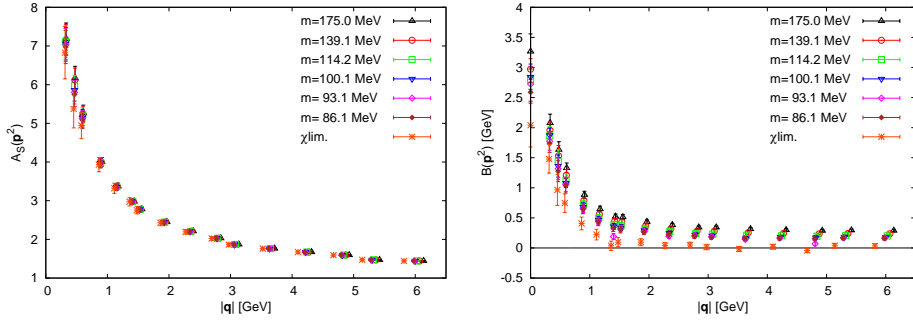
Fig. 2. *Spatial component* $A_S(\mathbf{p})$ *(l.h.s.) and scalar component* $B(\mathbf{p})$ *(r.h.s) for several quark masses* m *and in the chiral limit.*
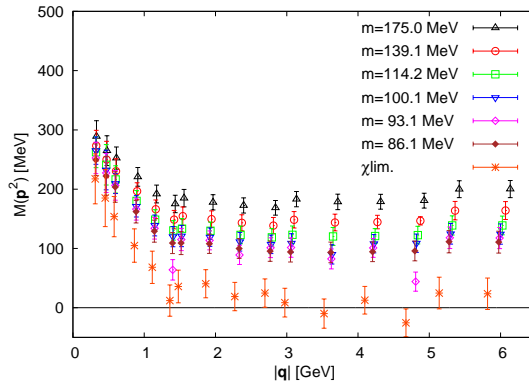
Fig. 3. *Dynamical mass function* $M(\mathbf{p})$ *for several quark masses* m *and in the chiral limit.*

References

1. C. Feuchter and H. Reinhardt, Phys. Rev. D **70**, 105021 (2004) [hep-th/0408236].
2. M. Pak and H. Reinhardt, Phys. Lett. B **707**, 566 (2012) [arXiv:1107.5263 [hep-ph]].
3. M. Pak and H. Reinhardt, Phys. Rev. D **88**, 125021 (2013) [arXiv:1310.1797 [hep-ph]].
4. G. Burgio, M. Schröck, H. Reinhardt and M. Quandt, Phys. Rev. D **86**, 014506 (2012) [arXiv:1204.0716 [hep-lat]].
5. F. D. R. Bonnet *et al.* [CSSM Lattice Collaboration], Phys. Rev. D **65**, 114503 (2002) [hep-lat/0202003].
6. J. B. Zhang *et al.* [CSSM Lattice Collaboration], Phys. Rev. D **70**, 034505 (2004) [hep-lat/0301018].
7. H. Neuberger, Phys. Lett. B **417**, 141 (1998) [hep-lat/9707022].
8. P. Hasenfratz, V. Laliena and F. Niedermayer, Phys. Lett. B **427**, 125 (1998) [hep-lat/9801021].

9. R. G. Edwards *et al.* [SciDAC and LHPC and UKQCD Collaborations], Nucl. Phys. Proc. Suppl. **140**, 832 (2005) [hep-lat/0409003].
10. F. Winter, PoS LATTICE **2013**, 042 (2013).
11. F. T. Winter, M. A. Clark, R. G. Edwards and B. Joó, arXiv:1408.5925 [hep-lat].
12. M. Lüscher and P. Weisz, Commun. Math. Phys. **97**, 59 (1985) [Erratum-ibid. **98**, 433 (1985)].
13. G. Burgio, M. Quandt and H. Reinhardt, Phys. Rev. Lett. **102**, 032002 (2009) [arXiv:0807.3291 [hep-lat]].
14. J. I. Skullerud and A. G. Williams, Nucl. Phys. Proc. Suppl. **83**, 209 (2000) [hep-lat/9909142].
15. R. Alkofer and P. A. Amundsen, Nucl. Phys. B **306**, 305 (1988).
16. C. B. Lang and M. Schröck, Phys. Rev. D **84**, 087704 (2011) [arXiv:1107.5195 [hep-lat]].
17. L. Y. Glozman, C. B. Lang and M. Schröck, Phys. Rev. D **86**, 014507 (2012) [arXiv:1205.4887 [hep-lat]].
18. Y. Delgado Mercado, M. Pak and M. Schröck, in preparation.

Constituent-Quark Masses and Baryon Spectroscopy

W. Plessas

Theoretical Physics, Institute of Physics, University of Graz, A-8010 Graz, Austria

Abstract. We discuss the hierarchy of constituent quark masses prevailing in effective models of quantum chromodynamics, specifically in the relativistic constituent-quark model. We observe that the dynamical mass gain over current-quark masses is more or less independent of the quark flavor and amounts to about $\Delta m \approx 370 \pm 30$ MeV. Similar values are also supported by alternative effective descriptions of baryon spectroscopy such as the Dyson-Schwinger approach.

The modern constituent-quark model has turned out to be quite successful as an effective tool to describe a variety of baryon properties and reactions [1]. It considers baryons as relativistic bound states of three constituent quarks Q interacting mutually. The Q-Q forces rely on a confinement and a hyperfine interaction. In such a framework constituent quarks are to be considered as quasi-particles whose masses are generated dynamically. The spontaneous breaking of chiral symmetry (SBχS) of low-energy quantum chromodynamics (QCD) is generally assumed to be responsible for attributing mass to constituent quarks.

We have set up a relativistic constituent-quark model (RCQM) covering all known baryons with flavors u, d, s, c, and b in a universal framework [2–4]. It relies on a relativistically invariant mass operator containing a linear confinement interaction, according to the string tension of QCD, and a hyperfine interaction, representing the exchange of pseudoscalar Goldstone bosons in the regime of SBχS of low-energy QCD. The model contains a total of 13 input parameters, of which 10 are assumed as predetermined or taken as educated guesses and only three are considered as really open fit parameters; the latter are determined by a best fit of the baryon spectra (for details see Refs. [2] or [5]).

Among the input parameters we also find the masses of the constituent quarks of flavors u, d, s, c, and b. While the masses of the light-flavored constituent quarks are set to the traditional values of $m_u = m_d \approx 300$ MeV, the magnitudes of the constituent-quark masses of the other flavors s, c, and b are determined such as to best reproduce the lowest lying baryons containing one of these flavors, i.e. Λ, Λ_c, and Λ_b. This leads to the hierarchy of constituent quark masses given in the third column of the Table.

It is immediately evident that the dynamical mass gains of constituent quarks over current quarks scatter around a value of ~370 MeV for all flavors in the RCQM. This is to some extent surprising, since for heavier flavors the transition from current to constituent quarks has usually been considered as insignificant. We emphasize, however, that the values of the constituent-quark masses

Quark flavor	PDG [6] m_q	RCQM [2,5] m_Q	Δm	DSE [7] Δm
$\frac{1}{2}(u+d)$	$3.3 - 4.2$	340	~ 336	~ 276
s	95 ± 5	480	~ 385	~ 278
c	1275 ± 25	1675	~ 400	~ 330
b	4660 ± 30	5055	~ 395	~ 400

Table 1. Masses of current quarks q and constituent quarks Q as well as their differences $\Delta m = m_Q - m_q$ for the flavors u, d, s, c, and b, as found in the RCQM and DSE approaches.

as quoted in the Table are essential for the RCQM to reproduce the phenomenological spectra of all known baryons in good quality. Furthermore, the magnitudes Δm occurring in the RCQM compare reasonably well with the quark-mass gains towards low momenta obtained in the relativistic framework of Dyson-Schwinger equations (DSE), as followed, e.g., in Ref. [7]. Only, the latter fall a bit lower and stretch over a wider range, namely, $\Delta m \approx 340 \pm 60$ MeV.
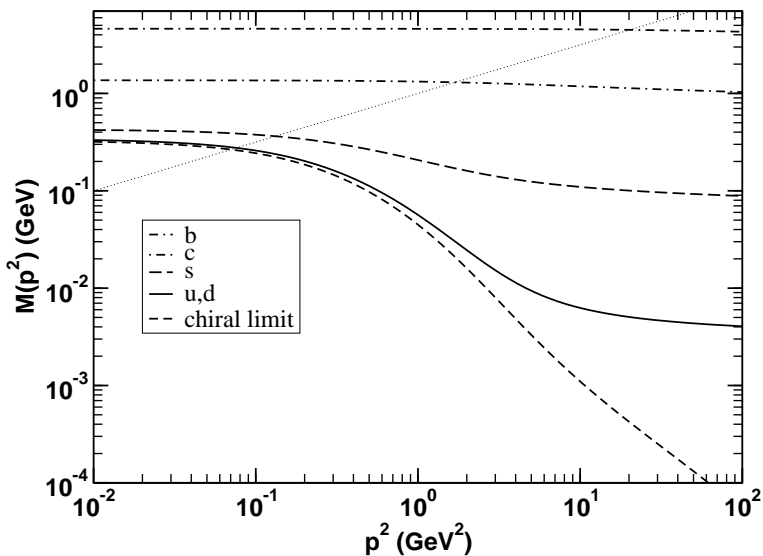
Fig. 1. Momentum dependence of quark masses from the DSE approach [7]. Figure by courtesy from A. Krassnigg.

The generation of constituent-quark masses can nicely be followed in the DSE approach. From the Figure it is seen, how the dynamical mass is acquired, when going from higher momenta (current quarks) to lower momenta (constituent quarks). For the various flavors mass gains are obtained as quoted in the last column of the Table. The phenomenon is even observed with approximately the same result, when starting from the chiral limit of $m_q = 0$. One may thus expect

a common reason for all flavors to develop a similar mass gain in the transition from current to constituent quarks.

We note that a similar investigation of the pattern of constituent-quark masses has been done by M. Rosina, including evidences from even other effective approaches to low-energy QCD, employing the notion of constituent quarks. The evidences he found are basically in line with the ones presented here [8].

While the hierarchy of constituent-quark masses has been discussed here by evidences from baryon spectroscopy, it should be mentioned that the same RCQM, with the $Q-Q$ hyperfine interaction based on Goldstone-boson exchange is also capable of describing the baryon electroweak structures (see, e.g., Refs. [1] or [9]), gravitational form factors [5], and a series of other baryon observables [10, 11] in good agreement with phenomenology and in cases, where experimental data are missing, in concordance with results from lattice QCD.

In summary it remains as a challenge to determine the very dynamical ingredients for generating constituent-quark masses. Several possibilities are offered in the literature for producing quasi-particles. None has hitherto been carried out to such an extent or is conclusive insofar as to provide an explanation of the constituent-quark masses of all flavors u, d, s, c, and b in QCD.

Acknowledgment

References

1. W. Plessas, PoS LC **2010**, 017 (2010); arXiv:1011.0156 [hep-ph]
2. J. P. Day, W. Plessas, and K. S. Choi, arXiv:1205.6918 [hep-ph]
3. J. P. Day, K. S. Choi, and W. Plessas, Few-Body Syst. **54**, 329 (2013)
4. J. P. Day, W. Plessas, and K. S. Choi, in: *Looking into Hadrons* (Proceedings of the Mini-Workshop, Bled, Slovenia, 2013), ed. by B. Golli, M. Rosina, and S. Sirca. DMFA, Ljubljana (2013); p. 6
5. J. P. Day, PhD Thesis, University of Graz (2013)
6. K. A. Olive *et al.* [Particle Data Group Collaboration], Chin. Phys. C **38**, 090001 (2014)
7. A. Höll, A. Krassnigg, C. D. Roberts, and S. V. Wright, Int. J. Mod. Phys. A **20**, 1778 (2005); arXiv:nucl-th/0411065
8. M. Rosina, private communication and contribution to these proceedings
9. M. Rohrmoser, K. S. Choi, and W. Plessas, Acta Phys. Polon. Supp. **6**, 371 (2013)
10. T. Melde, L. Canton, and W. Plessas, Phys. Rev. Lett. **102**, 132002 (2009)
11. T. Melde, W. Plessas and B. Sengl, Phys. Rev. D **77**, 114002 (2008)

Lambda-nucleus versus nucleon-nucleus potential

Bogdan Povh[a] and Mitja Rosina[b,c]

[a]Max-Planck-Institut für Kernphysik, Postfach 103980, D-69029 Heidelberg, Germany
[b]Faculty of Mathematics and Physics, University of Ljubljana, Jadranska 19, P.O. Box 2964, 1001 Ljubljana, Slovenia
[c]J. Stefan Institute, 1000 Ljubljana, Slovenia

Abstract. We are exploring a plausible mechanism why the Λ hyperon feels twice weaker mean field of a nucleus ($\sim$ -27 MeV) compared to a nucleon ($\sim$ -50 MeV).

1   Introduction

The depth of the potential which the Λ baryon is feeling in the nucleus is surprisingly independent of the nucleus in the whole region from the light to the heavy nuclei. Its value -27 MeV has been deduced from the $\pi^+ + A \rightarrow K^+ + _\Lambda A$ experiments. This number should be compared to the potential depth for the nucleon in the nucleus of about -50 MeV. The nuclear potential for the nucleons is less accurate than that for Λ because it cannot be measured for strongly bound nucleons. In fact, the Λ baryon in a nucleus is the best demonstration of the nuclear potential well.

2   Asumptions

1. The mean field of an isospin symmetric nucleus consists of an attractive σ-field and a repulsive ω-field. The former is a Lorentz scalar and the latter is a zero-component of a Lorentz four-vector.
2. We represent σ as a two-pion system and ω as a three-pion system.
3. Both fields are coupled to the probe (Λ or N) via pions.
4. Pions are coupled directly to quarks and not to an "elementary" baryon.
5. The strange quark has no pion cloud and no pion coupling.
6. We assume that the dominant "pion cloud" can be written as s one-pion and two-pion admixtures to bare quarks. The corresponding amplitude squared $a \approx 0.18$ has been determined from several nucleon observables in our previous papers [1–4] describing constituent quarks u and d as composites of bare quarks **u**, **d** and pions:

$$|u\rangle = \sqrt{(1 - \frac{3}{2}a - -\frac{3}{2}a^2)}\,|\mathbf{u}\rangle - \sqrt{a}|\mathbf{d}\pi^+\rangle + \sqrt{\frac{a}{2}}\,|\mathbf{u}\pi^0\rangle + a\,|\mathbf{u}(\pi^+\pi^- - \pi^0\pi^0/\sqrt{2})\rangle,$$

$$|d\rangle = \sqrt{(1 - \frac{3}{2}a - -\frac{3}{2}a^2)}\,|\mathbf{d}\rangle + \sqrt{a}\,|\mathbf{u}\pi^-\rangle - \sqrt{\frac{a}{2}}\,|\mathbf{d}\pi^0\rangle + a\,|\mathbf{d}(\pi^+\pi^- - \pi^0\pi^0/\sqrt{2})\rangle.$$

7. The coupling constant to the effective two pion fluctuation was assumed to be the square of the coupling constant for the single pion

3   The σ-field

The σ-field is proportional to the coupling of the two pions to quarks. Since we consider the ratio between the Λ-nucleus potential and the N-nucleus potential, rather than their absolute values, the proportionality constant cancels.

3.1   One-pion admixtures

The contribution comes from two different quarks. The probe (proton or neutron) feels the σ-part of the potential proportional to the amplitude

$$A^N_{\sigma,1} = \langle p\sigma|p\rangle = \langle p(\sqrt{\tfrac{2}{3}}\pi^+\pi^- - \sqrt{\tfrac{1}{3}}\pi^0\pi^0)|p\rangle = -(\sqrt{\tfrac{2}{3}} - \tfrac{1}{2}\sqrt{\tfrac{1}{3}})\,(1 - \tfrac{3}{2}a - \tfrac{3}{2}a^2)\,a$$

$$= -0.064.$$

It is interesting that the probe Λ feels the same amplitude $A^\Lambda_{\sigma,1} = A^N_{\sigma,1}$! It is also interesting to note that this contribution, though small, is repulsive.

3.2   Two-pion admixtures

In this case, the contribution comes only from the same quark. Since the two-pion dressing of each quark is isoscalar, the u and d quarks contribute the same amplitude, and the s quark contributes nothing. Therefore Λ feels onli 2/3 of this contribution compared to the nucleon.

$$A^N_{\sigma,2} = 3 \times \sqrt{\tfrac{2}{3}}\sqrt{(1 - \tfrac{3}{2}a - \tfrac{3}{2}a^2)}\,(a + \tfrac{1}{2}a) = 0.546\,,$$

$$A^\Lambda_{\sigma,2} = 2 \times \sqrt{\tfrac{2}{3}}\sqrt{(1 - \tfrac{3}{2}a - \tfrac{3}{2}a^2)}\,(a + \tfrac{1}{2}a) = 0.364\,.$$

The total contribution is then

$$A^N_\sigma = A^N_{\sigma,1} + A^N_{\sigma,2} = 0.482\,, \qquad A^\Lambda_\sigma = A^\Lambda_{\sigma,1} + A^\Lambda_{\sigma,2} = 0.300\,.$$

4   Discussion

The nuclear binding is a fundamental question of the nuclear physics and requires a proper explanation.

In the early days of the hypernuclear spectroscopy Dalitz and von Hippel [5] suggested that the Λ may be contaminated by an admixture of the Σ plus pion. More recently, excited states of several light hypernuclei have been studied by the gamma spectroscopy. In the present analysis of the excited states in the light hypernuclei the admixture of a Σ in the Λ has been estimated to be less than

1% [6]. Therefore the two pion exchange via virtual Σ cannot be the explanation of the large Λ binding in the nucleus. Consequently also the two pion exchange via the virtual delta excitation is not very likely the proper explanation of the nucleon binding in the nucleus.

In the present paper we discuss a model which gives a proper ratio of the two bindings, for the nucleon and for the Λ. The two-pion admixtures suggest the ratio between the Λ-nucleus potential and the N-nucleus potential around 2/3. There is a slight destructive interference between two-pion and one-pion contributions which brings the Λ/N ratio from 2/3 sligtly towards 1/2 , but not enough. The contribution of the repulsive ω-field turns out to be small in the proposed model and we ignore it.

References

1. M. Rosina and B. Povh, Bled Workshops in Physics **14** (2013) No.1, 52-56; also available at http://www-f1.ijs.si/BledPub.
2. B. Povh and M. Rosina, Bled Workshops in Physics **12** (2011) No.1, 82-87; also available at http://www-f1.ijs.si/BledPub.
3. B. Povh and M. Rosina, arXiv:1107.5977 (hep-ph).
4. A. Bunyatyan and B. Povh, Eur. Phys. J. A **27** (2006) 359-364.
5. R. H. Dalitz and F. von Hippel, Phys.Lett. **19** (1964)) 153.
6. E. Hiyama, H. Nemura, A. Nogga, private communication.

News from Belle: selected spectroscopy results

M. Bračko[a,b]

[a] University of Maribor, Smetanova ulica 17, SI-2000 Maribor, Slovenia
[b] Jožef Stefan Institute, Jamova cesta 39, SI-1000 Ljubljana, Slovenia

Abstract. This paper reports on selected recent results from the spectroscopy measurements performed with the experimental data collected by the Belle spectrometer, which has been operating at the KEKB asymmetric-energy e^+e^- collider in the KEK laboratory in Tsukuba, Japan.

1 Introduction

The Belle detector [1] at the asymmetric-energy e^+e^- collider KEKB [2] was operating between 1999 and 2010. During this time, the experiment has accumulated about 1 ab^{-1} of data. The KEKB collider, often called a *B-factory*, because for the most of its time it was operating around the $\Upsilon(4S)$ resonance, thus enabling Belle experiment to collect a sample of about 772 million pairs of $B\bar{B}$ mesons. However, the experiment has also accumulated substantial data samples at other Υ resonances, like $\Upsilon(1S)$, $\Upsilon(2S)$ and $\Upsilon(5S)$, as well as in the nearby continuum. In particular, the data samples at the $\Upsilon(4S)$ and $\Upsilon(5S)$ resonances are by far the largest available in the world, corresponding to integrated luminosities of 800 fb^{-1} and 123 fb^{-1}, respectively [3]. Large amount of collected experimental data and excellent detector performance enabled many interesting spectroscopic results, including discoveries of new charmonium(-like) and bottomonium(-like) hadronic states and studies of their properties. This report focuses on some of these results that triggered more interest at the workshop.

2 Charmonium and Charmonium-like States

There has been a renewed interest in charmonium spectroscopy since 2002. The attention to this field was first drawn by the discovery of the two missing $c\bar{c}$ states below the open-charm threshold, $\eta_c(2S)$ and $h_c(1P)$ [4,5] with $J^{PC}=0^{-+}$ and 1^{+-}, respectively, but even with the discoveries of new charmonium-like states (so called "XYZ" states).

2.1 The $X(3872)$ news

The story about the so called "XYZ" states began in 2003, when Belle reported on $B^+ \to K^+ J/\psi\pi^+\pi^-$ analysis, where a new state decaying to $J/\psi\pi^+\pi^-$ was discovered [7]. The new state, called X(3872), was soon confirmed and also intensively

studied by the CDF, DØ and *BABAR* collaborations [8–17, 19–21], and recently also by the LHC experiments [22, 23]. So far it has been established that this narrow state ($\Gamma = (3.0^{+1.9}_{-1.4} \pm 0.9)$ MeV) has a mass of (3872.2 ± 0.8) MeV, which is very close to the $D^0\overline{D}^{*0}$ threshold [6]. Intensive studies of several X(3872) production and decay modes were performed by Belle and other experiments to determine the X(3872) properties. These studies suggested two possible J^{PC} assignments, 1^{++} and 2^{-+}, and establish the X(3872) as a candidate for a loosely bound $D^0\overline{D}^{*0}$ molecular state. However, results provided substantial evidence that the X(3872) state must contain a significant $c\bar{c}$ component as well.

As mentioned above, the Belle experiment has already finished collecting data and the final measured sample still does not allow Belle to completely distinguish between the two possible J^{PC} assignments, 1^{++} and 2^{-+}, although the latter case is not very likely. This was confirmed in 2013, when the quantum-number-assignment issue was finally resolved by the LHCb experiment [24]. They performed a full five-dimensional amplitude analysis of the angular correlations between the decay products in $B^+ \rightarrow X(3872)K^+$ decays, where X(3872) $\rightarrow J/\psi\pi^+\pi^-$ and $J/\psi \rightarrow \mu^+\mu^-$, they unambiguously determined 1^{++} assignment. This result also favours exotic explanations of the X(3872) state.

3   Summary and Conclusions

Many new particles have already been discovered during the operation of the Belle experiment at the KEKB collider, and some of them are mentioned in this report. Some recent Belle results also indicate that analogs to exotic charmonium-like states can be found in $b\bar{b}$ systems. Although the operation of the experiment has finished, data analyses are still ongoing and therefore more interesting results on charmonium(-like) and bottomonium(-like) spectroscopy can still be expected from Belle in the near future. These results are eagerly awaited by the community and will be widely discussed at various occassions, in particular at workshops and conferences.

References

1. Belle Collaboration, *Nucl. Instrum. Methods* A **479**, 117 (2002).
2. S. Kurokawa and E. Kikutani, *Nucl. Instrum. Methods* A **499**, 1 (2003), and other papers included in this Volume.
3. J. Brodzicka *et al.*, *Prog. Theor. Exp. Phys.* , 04D001 (2012).
4. Belle Collaboration, *Phys. Rev. Lett.* **89**, 102001 (2002).
5. Cleo Collaboration, *Phys. Rev. Lett.* **95**, 102003 (2005).
6. K.A. Olive *et al.* (Particle Data Group), *Chin. Phys. C* **38**, 090001 (2014).
7. Belle Collaboration, *Phys. Rev. Lett.* **91**, 262001 (2003).
8. CDF Collaboration, *Phys. Rev. Lett.* **93**, 072001 (2004); DØ Collaboration, *Phys. Rev. Lett.* **93**, 162002 (2004); *BABAR* Collaboration, *Phys. Rev.* D **71**, 071103 (2005).
9. Belle Collaboration, arXiv:hep-ex/0505037, arXiv:hep-ex/0505038; submitted to the Lepton-Photon 2005 Conference.
10. Belle Collaboration, *Phys. Rev. Lett.* **97**, 162002 (2006).

11. *BABAR* Collaboration, *Phys. Rev.* D **74**, 071101 (2006).
12. Belle Collaboration, arXiv:0809.1224v1 [hep-ex]; contributed to the ICHEP 2008 Conference.
13. Belle Collaboration, arXiv:0810.0358v2 [hep-ex]; contributed to the ICHEP 2008 Conference.
14. CDF Collaboration, *Phys. Rev. Lett.* **98**, 132002 (2007).
15. *BABAR* Collaboration, *Phys. Rev.* D **77**, 011102 (2008).
16. *BABAR* Collaboration, *Phys. Rev. Lett.* **102**, 132001 (2009).
17. Belle Collaboration, *Phys. Rev. Lett.* **107**, 091803 (2011).
18. E. S. Swanson, *Phys. Rep.* **429**, 243 (2006).
19. Belle Collaboration, *Phys. Rev.* D **84**, 052004(R) (2011).
20. CDF Collaboration, *Phys. Rev. Lett.* **103**, 152001 (2009).
21. *BABAR* Collaboration, *Phys. Rev.* D **77**, 111101(R) (2008).
22. LHCb Collaboration, *Eur. Phys. J.* C **72**, 1972 (2012).
23. CMS Collaboration, *J. High Energy Phys.* **04**, 154 (2013).
24. LHCb Collaboration, *Phys. Rev. Lett.* **110**, 222001 (2013).

The constituent quark as a soliton in chiral quark models

Bojan Golli

Faculty of Education, University of Ljubljana, 1000 Ljubljana, Slovenia and Jožef Stefan Institute, 1000 Ljubljana, Slovenia

Abstract. We discuss the possibility that the soliton carrying the baryon number 1/3, obtained in the linear σ-model and in the Nambu – Jona-Lasinio model can be identified with the constituent quark. In the linear σ-model we have derived meson exchange potentials between two solitons which turn out to resemble potentials used in constituent quark models.

The mechanism in which a nonstrange constituent quark acquires its mass ∼ $350 - 400$ MeV is phenomenologically described via spontaneous breaking of chiral symmetry. Yet, such a structureless particle does not agree with a picture of the constituent quark as an extended object in which the quark is surrounded by a cloud of quark-antiquark (meson) and gluon excitations. The fact that the scale for chiral symmetry breaking appears at lower energies than the confinement scale supports a model in which the constituent quark is represented by a current quark surrounded by a chiral field rather than a gluon field, as first suggested by Georgi and Manohar [1], and further elaborated by Cheng and Li [2], and by Baumgartner, Pirner, Königsmann and Povh [3] (see also the contribution of M. Rosina in these Proceedings [4]).

One of the simplest models describing the spontaneous breaking of chiral symmetry is the linear σ-model (LSM). In the non-strange sector it involves u and d quarks, a triplet of pions and the σ-meson [5–8]. The model possesses, for sufficiently strong pion-quark coupling constant g, soliton solutions obtained by putting three quarks in the lowest 1s orbit and allowing for nonzero pion field around the quark source. Below the critical coupling constant only free Dirac particles of mass $M = gf_\pi$ exist, f_π being the pion decay constant. We found [9] another type of non-trivial solutions by putting only one quark in the lowest orbit which we identified with the constituent quark.

In figure 1a) the energy of such a quark soliton is displayed as a function of $M = gf_\pi$. For comparison, the energy of the three quark soliton (the nucleon soliton) divided by 3 is also shown. The three quarks in the nucleon soliton generate a stronger chiral field than in the single quark soliton and the resulting attractive potential lowers more substantially the energy of the valence orbit (ε_{val}) producing a large gap between the two solutions. The energy of the quark soliton is higher than the popular value of the constituent quark mass. In our calculation
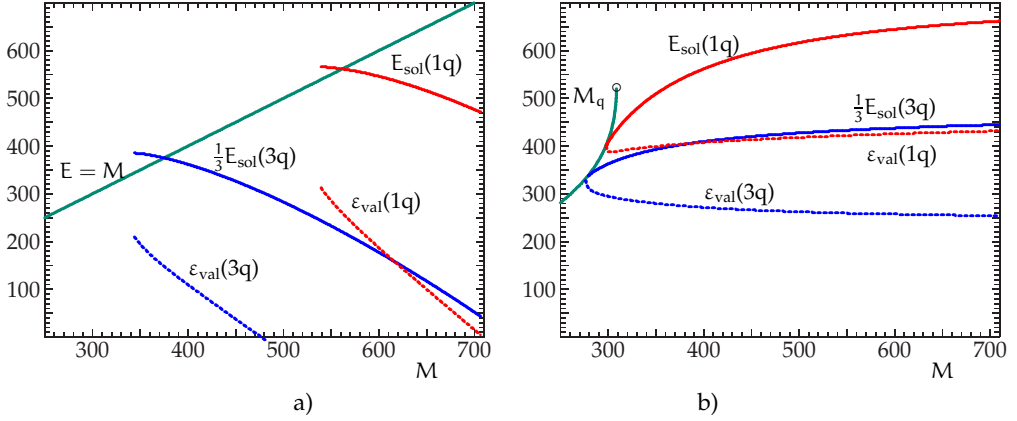
Fig. 1. (a) (b)

we do project the solution onto the subspace of good angular momentum and isospin, but we do not perform the projection onto the states with good linear momentum. The solution is thus interpreted as a wave packet of states with good linear momenta; projecting out the zero-momentum state would further lower the energy of the soliton. Let us notice that for both solutions the valence orbit sinks into the Dirac sea at a sufficiently large coupling constant producing a topological soliton (Skyrmion).

From our solution it is possible to derive a potential between two quark solitons in the framework of the Born Oppenheimer approximation. The interesting part of the interaction is the pion exchange potential. The pion field around the quark soliton with good angular momentum and isospin can be written in the form:

$$\vec{\pi}_b(\mathbf{r}) = \frac{1}{3}\pi(r)\,\hat{\mathbf{r}}\cdot\boldsymbol{\Sigma}_b\,\vec{T}_b\;, \tag{1}$$

where $\boldsymbol{\Sigma}$ and $\vec{T}$ act on spin and isospin of the quark soliton, respectively. To obtain the potential between two such solitons, one at the origin and the other one at position $\mathbf{r}$, we evaluate the quark-meson and the meson-meson interaction for such a configuration. For the quark-pion interaction we obtain

$$V_\pi^q(r) = \frac{2g}{3}\langle Q|\sigma_0\tau_0|Q\rangle \int d^3\mathbf{r}'u(r')v(r')\,\pi(|\mathbf{r}-\mathbf{r}'|)\,\hat{\mathbf{r}}'\cdot\boldsymbol{\Sigma}_a\,\widehat{(\mathbf{r}-\mathbf{r}')}\cdot\boldsymbol{\Sigma}_b\,\vec{T}_a\vec{T}_b\;, \tag{2}$$

where σ_0 and τ_0 now act on current quark spin and isospin. A similar expression is obtained from the meson self-interaction ("Mexican hat"). The potential (2) contains the scalar as well the tensor part. The scalar part is displayed in figure 2 and compared to a typical one-pion exchange potentials used in the constituent quark model calculations. The potential satisfies $\int dr\, r^2 V_\pi(r) = 0$, a constraint that has to be fulfilled for any pseudo-scalar exchange potentials. It has the correct asymptotic behavior leading to the appropriate form of the pion-exchange potential between two nucleons. The attractive part is too shallow and has a too large range which could be attributed to the spurious center-of-mass motion. We expect that
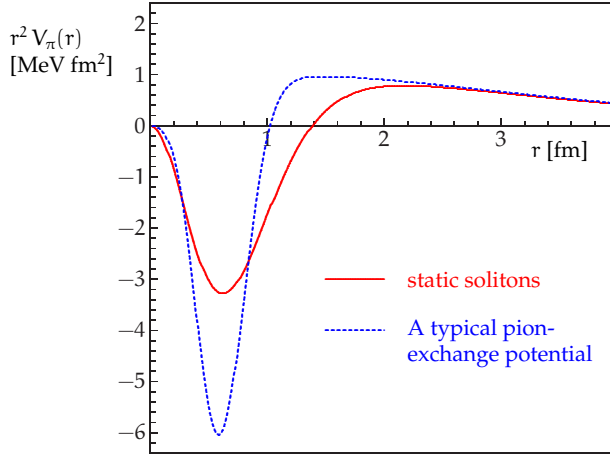
Fig. 2. The pion exchange effective potential (multiplied by r^2) between two quark solitons for $M = 560$ MeV (solid line) compared to a typical OPEP.

linear momentum projection would reduce its range and through the above integral constraint lower the depth of the attractive part, which could finally bring our prediction closer to a realistic OPEP.

Our model of the constituent quark is further supported by our finding that similar quark solitons exist also in a more fundamental chiral model, the Nambu – Jona-Lasinio (NJL) model. In this model the sigma and pion fields are related to the quark-antiquark excitations of the Dirac sea by

$$\sigma(r) = \sum_{\varepsilon_j < 0} \bar{q}_j q_j \, \mathcal{R} \,, \qquad \boldsymbol{\pi}(\mathbf{r}) = \sum_{\varepsilon_j < 0} \bar{q}_j i\gamma_5 \boldsymbol{\tau} q_j \, \mathcal{R}$$

where $\mathcal{R}$ denotes a regulator which is needed to regularize the ultraviolet divergences, and introduces a new parameter, the cut-off. In our calculation [10, 11] we used a version of the model in which the interaction between quarks is induced by the instantons [12] and has a finite range. The mass of the "bare" constituent quark M which is equal to gf_π in the linear σ-model is now substituted by the 4-momentum-dependent mass $M \to M\mathcal{R}(k^2)$, $k^2 = \mathbf{k}^2 - E^2$; M remains in the model as a (free) parameter measuring the strength of the σ-field in the vacuum. The pole of the quark propagator is obtained by solving the condition $k^2 + M^2\mathcal{R}(k^2) = 0$. The solution exists only below a certain value of M. Using $\mathcal{R}(k^2) = e^{-k^2/\Lambda^2}$ and fixing the cut-off parameter Λ to reproduce the pion decay constant, the critical value of M is around 300 MeV. Above this value only solutions with non-trivial values of chiral fields exist. Similarly as in the linear σ-model, putting three quarks in the valence orbit a soliton corresponding to the nucleon emerges; if we put only one quark in the valence orbit, we obtain a solitonic solution which we identify with the constituent quark.

The energies of both solutions as functions of M are displayed in figure 1b) in the same way as the analogous solutions in the linear σ-model. The energy of the " bare" constituent quark is denoted by M_q; in contrast to the LSM this

solution smoothly continues into the soliton solution. Interestingly, the solutions of both models have similar energies, however, the energies in the NJL model raise with M while those in the LSM lower. This is a consequence of the regularization of the valence orbit which is not performed in the LSM as well in other versions of the NJL model. The regularization used in our approach prevents the orbit to shrink below a certain size and thus makes the soliton absolutely stable without any further ad hoc constraint. The energy of the valence orbit remains almost constant with M and does not sink into the Dirac sea. The presence of the time variable in the regulator does not allow us to perform the exact angular and linear momentum projection which would lower the soliton energy further, and eventually bring it in the ball park of values used in the constituent quark model calculations.

References

 1. A. Manohar and H. Georgi, Nucl. Phys. B234 (1984) 189.
 2. T. P. Cheng and Ling-Fong Li, Phys. Rev. Lett. 74 (1995) 2872.
 3. S. Baumgartner, H. J. Pirner, K. Königsmann and B. Povh, Z. Phys. A 353 (1996) 397.
 4. M. Rosina, these Proceedings.
 5. M. Gell-Mann and M. Lévy, Nuovo Cim. **16** (1960) 705.
 6. M. C. Birse and M. K. Banerjee, Phys. Lett. B 136 (1984) 284; Phys. Rev. D 31 (1985) 118.
 7. S. Kahana, G. Ripka and V. Soni, Nucl. Phys. A 415 (1984) 351.
 8. B. Golli and M. Rosina, Phys. Lett. B 165 (1985) 347.
 9. B. Golli and M. Rosina, Phys. Lett. B 393 (1997) 161.
10. B. Golli, W. Broniowski, and G. Ripka: Phys. Lett. **B437**, 24 (1998)
11. W. Broniowski, B. Golli, and G. Ripka: Nucl. Phys. **A703**, 667 (2002)
12. D. I. Diakonov and V. Y. Petrov, Nucl. Phys. B 272 (1986) 457

Positive parity D_s mesons and Z_c^+ from lattice QCD

Luka Leskovec

Jozef Stefan Institute, Jamova 39, 1000 Ljubljana, Slovenia

Abstract. Two particularly interesting channels are presented: the positive parity D_s mesons and the exotic Z_c^+. In the D_s channel there was some tension between experiment and theory, as the $D_{s0}^*(2317)$ and $D_{s1}(2460)$, which were experimentally found below the DK and D^*K thresholds respectively, were theoretically supposed to be above threshold. We perform a lattice QCD simulation where we include not only $\bar{c}s$ but also $D^{(*)}K$ operators; this enables us to take into account the threshold effects. The extracted mases are found below threshold and match experimental values within error. We perform also a lattice QCD simulation of the exotic Z_c^+ channel, where experiments found several manifestly exotic states with at least two quark and two anti-quarks. In the operator basis we include all relevant scattering operators $J/\psi\pi, \eta_c\rho, DD^*, \psi(2S)\pi, D^*D^*, \psi(3770)\pi, \psi_{3^{--}}\pi$ as well as additional diquark anti diquark operators. We are able to identify all scattering levels within the energy region of interest, however no additional level identifiable as a candidate for Z_c^+ is found.

Lattice QCD is the theory of the Strong interaction formulated in discrete Euclidean space time, specifically within a finite sized box with periodic boundary conditions. The pre-eminent advantage of lattice QCD is that it allows the nonperturbative calculation of correlator functions of hadronic operators in terms of fundamental quark and gluon degrees of freedom. From these correlator functions, the spectrum of hadrons in a given quantum channel can be extracted. However unlike in the continuum, the spectrum from a lattice simulation is discrete due to the periodic boundary conditions in space. Here recent results from lattice simulations of the positive parity D_s mesons and the $J^{PC} = 1^{+-}$ charmonium channel are presented.

The positive parity D_s mesons, especially the $D_{s0}(2317)$ and $D_{s1}(2460)$, are understood quite badly from a theoretical point of view. Experimentally they are seen below the $D^{(*)}K$ thresholds [1], however neither quark models nor lattice QCD studies have been able to reproduce this so far [2]. Early quenched lattice studies, that ignored sea quark contributions only took into account $\bar{q}q$ operators and found results consistent with the quark model – $D_{s0}(2317)$ and $D_{s1}(2460)$ appeared above DK and D^*K thresholds respectively [3]. Dynamical studies followed, thinking that the issue might have been in the lack of sea quark contributions, however when pion and kaon masses were taken to be close to physical, the states of interest again appeared to be above their respective thresholds [4].

We performed dynamical lattice QCD simulations at two distinct pion masses, $m_\pi = 266$MeV and 156MeV, using both $\bar{c}s$ and $D^{(*)}K$ operators in the construction of the correlator matrix in order to take into the account the effects of the

threshold [5]. The discrete energy levels are in both cases obtained from the generalized eigenvalue problem [6]. When the scattering operators are not included in the analysis, we reproduce the previous results, where the $D_{s0}(2317)$ and $D_{s1}(2460)$ are above threshold. However when also the meson-meson scattering operators are included in the analysis, the above threshold energy level becomes two distinct levels - one above the respective threshold and one below. The Lüscher method [7,8] is used to obtain the phase shifts near and below threshold allowing to determine the position of the pole in the T matrix. We find [5] the $D_{s0}(2317)$ to be 78.9(5.4) MeV and 36.6(16.6) MeV below the DK threshold for the case of $m_\pi = 266$ MeV and the case of $m_\pi = 156$ MeV respectively. The $D_{s1}(2460)$ appears 93.2(4.7) MeV below threshold for $m_\pi = 266$ MeV and 44.2(9.9) MeV below threshold for $m_\pi = 156$ MeV. The lighter pion mass ensemble compares to experiment favorably: $m_{D_{s0}(2317)}^{exp} - m_K^{exp} - m_D^{exp} \approx 45.1$ MeV and $m_{D_{s1}(2460)}^{exp} - m_K^{exp} - m_D^{*exp} \approx 44.7$ MeV [1].

The $J^{PC} = 1^{+-}$ charmonium channel is interesting because experiments [9–11] recently discovered manifestly exotic hadrons – charged charmonium resonances. The first study of this channel [12], was focused on J/ψ and DD^* scattering below 4 GeV, however no candidate was found. Another study of this channel with lattice QCD appeared soon after, and was able to extract DD^* scattering parameters near threshold, however claimed to find no candidates for exotic hadrons [13].

We performed a comprehensive lattice QCD study of this channel using the ensemble with $m_\pi = 266$ MeV. In the construction of the correlator matrix operators corresponding to all scattering states relevant on the lattice below 4.3 GeV: $J/\psi\pi$, $\eta_c\rho$, DD^*, $\psi(2S)\pi$, D^*D^*, $\psi(3770)\pi$, $\psi_{3--}\pi$ as well as additional diquark anti-diquark operators, $[\bar{c}\bar{u}]_{3_c}[cu]_{\bar{3}_c}$ were used. The obtained discrete energy levels were identified with their respective scattering states and no additional state which could be identified as a candidate for the exotic hadron, was found under 4.2 GeV [14].

For the case of the positive parity D_s mesons we have resolved a long standing issue between experiment and theory, by taking into account the $D^{(*)}K$ threshold effects. In the charmonium channel we did not find any candidates for the exotic hadrons, even though we included explicit diquark anti-diquark operators in the analysis. Further and more extensive studies of this channel would need to be performed to shed some light on the theoretical understanding of the exotic hadrons in the $J^{PC} = 1^{+-}$ charmonium channel.

References

1. Particle Data Group, K. Olive *et al.*, Chin.Phys. **C38**, 090001 (2014).
2. S. Godfrey and N. Isgur, Phys.Rev. **D32**, 189 (1985).
3. R. Lewis and R. Woloshyn, Phys.Rev. **D62**, 114507 (2000), [arXiv:hep-lat/0003011].
4. D. Mohler and R. Woloshyn, Phys.Rev. **D84**, 054505 (2011), [arXiv:1103.5506].
5. C. Lang, L. Leskovec, D. Mohler, S. Prelovsek and R. Woloshyn, Phys.Rev. **D90**, 034510 (2014), [arXiv:1403.8103].
6. B. Blossier, M. Della Morte, G. von Hippel, T. Mendes and R. Sommer, JHEP **0904**, 094 (2009), [arXiv:0902.1265].
7. M. Luscher, Nucl.Phys. **B354**, 531 (1991).
8. M. Luscher, Nucl.Phys. **B364**, 237 (1991).
9. Belle Collaboration, Z. Liu *et al.*, Phys.Rev.Lett. **110**, 252002 (2013), [arXiv:1304.0121].
10. BESIII Collaboration, M. Ablikim *et al.*, Phys.Rev.Lett. **110**, 252001 (2013), [arXiv:1303.5949].
11. Belle Collaboration, K. Chilikin *et al.*, [arXiv:1408.6457].
12. S. Prelovsek and L. Leskovec, Phys.Lett. **B727**, 172 (2013), [arXiv:1308.2097].
13. Y. Chen *et al.*, Phys.Rev. **D89**, 094506 (2014), [arXiv:1403.1318].
14. S. Prelovsek, C. Lang, L. Leskovec and D. Mohler, [arXiv:1405.7623v2].

Constituent versus current quark masses

Mitja Rosina

Faculty of Mathematics and Physics, University of Ljubljana, Jadranska 19, P.O. Box 2964, 1001 Ljubljana, Slovenia
and J. Stefan Institute, 1000 Ljubljana, Slovenia

Abstract. It is an amazing fact that the difference between the current mass and the constituent mass (such as used in different constituent quark models) is almost constant from light to heavy quarks. It amounts to 330 MeV for u and d quarks and grows to 400-600 MeV for heavier quarks. The constituent quark mass is of course model-dependent and we review several models, the chromodielectric model, the linear sigma model and the Nambu–Jona-Lasinio model. They may give the clue which mechanism of dynamical mass generation is dominant in each case.

1 Difference between current and constituent masses

First we present the constituent quark masses for two different quark models in order to display their model-dependence as well as their dependence on the quark flavour.

	PDG	AL1	ΔAL1	Rel	ΔRel
u	2.3±0.6				
d	4.8±0.4				
$\frac{1}{2}$(u+d)	3.5±0.5	315	312	340	337
s	95±5	577	482	480	385
c	1275±25	1836	561	1675	400
b(1S)	4660±30	5227	567	5055	395

Table 1. PDG = current masses [1], AL1 = Grenoble AL1 parameters [2], Rel = Relativistic CQM [3], Δ = difference with respect to PDG.

2 Phenomenological determination of constituent quark masses

The concept of the constituent mass is model-dependent and makes sense only in its full context. As an illustration, we chose two different models; full details show that many fitted parameters are needed to cover many hadronic states with a "universal interaction". It is rewarding that both models suggest similar constituent masses.

2.1 Nonrelativistic constituent quark model with a two-body OGE potential

As an example, we choose the Grenoble AL1 potential [2]. The potential parameters and masses are fitted to reproduce a large body of baryonic and mesonic states.

$$V_{ij}^{AL1} = -\frac{\lambda_i^C}{2} \cdot \frac{\lambda_j^C}{2} \left(U_0 + \frac{\alpha}{r_{ij}} + \beta r_{ij} + \tilde{\alpha} \frac{2\pi\hbar^2}{3m_i m_j c^2} \frac{e^{-r_{ij}^2/r_0^2}}{\pi^{3/2} r_0^3} \sigma_i \cdot \sigma_j \right),$$

$$r_0(m_i, m_j) = A \left(\frac{m_i + m_j}{2m_i m_j} \right)^B, \qquad r_{ij} = |\mathbf{r}_i - \mathbf{r}_j|;$$

$m_b = 5227$ MeV, $\qquad m_c = 1836$ MeV, $\qquad A = 1.6553$ GeV^{B-1},
$m_s = 577$ MeV, $\qquad m_u = m_d = 315$ MeV, $\quad B = 0.2204$,
$U_0 = 624.075$ MeV, $\qquad \alpha = 74.895$ MeVfm,
$\beta = 629.315$ MeV/fm, $\quad \tilde{\alpha} = 274.948$ MeVfm.

2.2 Semirelativistic constituent quark model with a two-body confining+OGBE potential

The model has been developed and fitted by the Graz group [3] (for baryons only). Several levels, such as the Roper, are better fitted with the one-boson-exchange model than with the one-gluon-exchange model. However, the fit for the mesons is ambiguous if it is the mesons themselves that are exchanged.

$$H = \sum_{i=1}^{3} \sqrt{m_i^2 + k_i^2} + V^{conf}(\mathbf{r}_{ij}) + V^{hf}(\mathbf{r}_{ij}),$$

$$V^{conf} = B + Cr_{ij}, \quad V^{hf} = \left[V_{24}(\mathbf{r}_{ij}) \sum_{f=1}^{24} \lambda_i^f \lambda_j^f + V_0(\mathbf{r}_{ij}) \lambda_i^0 \lambda_j^0 \right] \sigma_i \cdot \sigma_j,$$

$$V_\beta = \frac{g_\beta^2}{4\pi} \frac{1}{12 m_i m_j} \left\{ \mu_\beta^2 \frac{\exp(-\mu_\beta r_{ij})}{r_{ij}} - \Lambda_\beta^2 \frac{\exp(-\Lambda_\beta r_{ij})}{r_{ij}} \right\}.$$

$m_b = 5055$ MeV, $\quad m_c = 1675$ MeV, $\qquad B = -402$ MeV,
$m_s = 480$ MeV, $\quad m_u = m_d = 340$ MeV, $\quad C = 2.33$ fm^{-2},
$g_{24}^2/4\pi = 0.7$, $\qquad \mu_{24} = 139$ MeV, $\qquad \Lambda_{24} = 700.5$ MeV,
$(g_0/g_{24})^2 = 1.5$, $\quad \mu_0 = 958$ MeV. $\qquad \Lambda_0 = 1484$ MeV.

3 The chromodielectric model

Assumption: The physical vacuum contains gluon condensate, it is dual super-conductive and does not transmit the color electric field. However, the color charges of quarks must drill a flux tube or a MIT-like bag in order to transmit field lines in a "perturbative vacuum", and that costs energy.

The chromodielectric "constant" χ (actually field) can be incorporated into the Lagrangian by the following transformation

$$A_a^\mu \to \chi B_a^\mu, \quad \partial_\mu \to \chi \partial_\mu, \quad \psi \to \psi/\sqrt{\chi}.$$

$$\mathcal{L} = -\tfrac{1}{4}\chi^4 B_a^{\mu\nu} B_{\mu\nu}^a + \bar{\psi}\left(\gamma^\mu(i\partial_\mu - gB_\mu \cdot \hat{C}) - \tfrac{m}{\chi}\right)\psi$$
$$+ \tfrac{1}{2}w^2(\chi\partial_\mu\chi)^2 - \tfrac{1}{8}M^2 w^2 \chi^2(2-\chi)^2.$$

For a qualitative feeling, we present a simple model with quark gas representing the nuclear matter [4]. The "current mass" $m = 20$ MeV is a model parameter, and the "constituent mass" $m/\chi = 160$ MeV comes out by minimization of energy and fitting model parameters to energy and density of nuclear matter.

4   The linear σ model

One usually describes the nucleon as a soliton of the Lagrangian

$$\mathcal{L} = i\bar{\psi}\gamma^\mu\partial_\mu\psi + g\bar{\psi}(\hat{\sigma} + i\boldsymbol{\tau} \cdot \hat{\boldsymbol{\pi}}\gamma_5)\psi + \tfrac{1}{2}\partial_\mu\hat{\sigma}\partial^\mu\hat{\sigma} + \tfrac{1}{2}\partial_\mu\hat{\boldsymbol{\pi}} \cdot \partial^\mu\hat{\boldsymbol{\pi}} - \mathcal{U}(\hat{\sigma}, \hat{\boldsymbol{\pi}})$$

For nucleon soliton, nucleon observables are well reproduced with $g = 6$.

Vacuum expectation value of σ is assumed to be f_π. Then, $gf_\pi \approx 550$ MeV acts as a mass term for the quark.

The question arises whether one might get a better description of the nucleon as a bound state of three one-quark solitons [5]. For $g > 6$, the quark soliton gets dressed in pions and its energy decreases. It reaches 350 MeV at $g = 9$ which is much too large. System of three separate quark solitons would become unstable and change into a nucleon soliton. Therefore it is better to stick to $g \sim 6$ and look for corrections. The "constituent mass" (soliton energy) will be reduced by three effects: (i) the linear momentum projection, (ii) additional pion loops (iii) the negative constant in the σ-exchange potential between such solitons.

For details see the contribution of B. Golli in these Proceedings [6].

5   The One-flavour Nambu–Jona-Lasinio Model

For pedagogical purposes, we have developed a very simple "two-level" version of the NJL model [7].

1. We assume a sharp 3-momentum cutoff $0 \leq |\mathbf{p}_i| \leq \Lambda$;
2. The space is restricted to a box of volume $\mathcal{V}$ with periodic boundary conditions. This gives a finite number of discrete momentum states,
   $\mathcal{N} = N_c N_f \mathcal{V}\Lambda^3/3\pi^2$ occupied by N quarks.
3. $|\mathbf{p}_i| \to P = \tfrac{3}{4}\Lambda$.
4. One flavour at a time.
5. When quarks scatter, they only change chirality (uper↔lower level) and conserve momenta.

$$H_{"NJL"} = \sum_{i=1}^{N} \left(\gamma_5(i)h(i)P + m_0\beta(i) \right)$$

$$- \frac{2G}{\mathcal{V}} \sum_{i=1}^{N} \sum_{\substack{j=1 \\ j \neq i}}^{N} \left(\beta(i)\beta(j) + \left(i\beta(i)\gamma_5(i) \right)\left(i\beta(j)\gamma_5(j) \right) \right).$$

We define

$$M = \sqrt{\left(E_g(N) - E_g(N-1) \right)^2 - P^2} = 335\,\mathrm{MeV}$$

$$Q = \langle\, g|\bar{\psi}\psi|g \,\rangle = \frac{1}{\mathcal{V}}\langle\, g| \sum_i \beta(i)|g \,\rangle = 250^3\,\mathrm{MeV}^3$$

$$m_\pi = E_1(N) - E_g(N) = 138\,\mathrm{MeV}\,.$$

The Hartree-Fock + RPA approximation (at large N) is very close to the accurate calculation and it gives

$$M - m_0 = \sqrt{\left(\frac{4}{\pi^2}\,G\Lambda^3 \right)^2 - \frac{(M-m_0)^2}{M^2}P^2}$$

$$Q = \frac{\Lambda^3}{\pi^2}\frac{M}{\sqrt{M^2+P^2}}$$

$$m_\pi \approx \sqrt{\sqrt{\frac{M^2+P^2}{M^2}}G\Lambda^3 m_0}\,.$$

$$\Lambda = 648\,\mathrm{MeV}, \quad G = 40.6\,\mathrm{MeV\,fm}, \quad m_0 = 4.58\,\mathrm{MeV}.$$

These values compare favourably with those of full Nambu-Jona Lasinio [8, 9]

$$\text{Coimbra}: \Lambda = 631\,\mathrm{MeV}, \quad G = 40\,\mathrm{MeV\,fm}, \quad m_0 \approx 5\,\mathrm{MeV},$$

$$\text{Buballa}: \Lambda = 664\,\mathrm{MeV}, \quad G = 37.8\,\mathrm{MeV\,fm}, \quad m_0 = 5.0\,\mathrm{MeV}.$$

Conclusion. If we assume that the NJL one-flavour interaction is the same for all quark flavours, due to the flavour independence of QCD, we see that $M - m_0$ really only slightly increases with the quark mass M (since the negative term $\frac{(M-m_0)^2}{M^2}P^2$ decreases).

References

1. K. A. Olive et al. (Particle Data Group), Chin. Phys. **C38**, 0900001 (2014) (URL: http://pdg.lbl.gov).
2. B. Silvestre-Brac, Few Body Systems **20**, 1 (1996).
3. J. P. Day, W. Plessas, Ki-Seok Choi, Bled Workshops in Phys.**13/1**,5 (2012); arXiv 1205.6918v1 (hep-ph).
4. M. Rosina, H.J. Pirner, Fizika (Zagreb) **19**, 2, 43-46 (1987) (Proc.Workshop on Mesonic Degrees of Freedom in Hadrons, Bled/Ljubljana 1987).
5. B. Golli and M. Rosina, Phys.Lett **B393**, 161-166 (1997).
6. B.Golli, these Proceedings.
7. M. Rosina and B. T. Oblak, Few-Body Syst.**47**, 117-123 (2010).
8. M. Fiolhais, J. da Providência, M. Rosina and C. A. de Sousa, Phys. Rev. C **56**, 3311 (1997).
9. M. Buballa, Phys. Reports **407**, 205 (2005).

Spin structure of ^{3}He studied by deuteron and nucleon knockout processes

S. Širca^{a,b}

^{a} Faculty of Mathematics and Physics, University of Ljubljana, Jadranska 19, 1000 Ljubljana, Slovenia
^{b} Jožef Stefan Institute, Jamova 39, 1000 Ljubljana, Slovenia

Abstract. In this talk we present a status report on several experiments performed recently in Hall A of the Thomas Jefferson National Accelerator Facility (TJNAF), i. e. Jefferson Lab (JLab) and within the A1 Collaboration at MAMI (Mainz). The common denominator of all these efforts is the study of spin structure of the ^{3}He nucleus in its ground state.

The following experiment have been covered:

1. JLab experiment E05-102 (co-spokespersons S. Gilad, D. W. Higinbotham, W. Korsch, B. Norum, S. Širca): *Measurement of double-spin asymmetries in the quasi-elastic* $^3\vec{\text{He}}(\vec{e}, e'd)p$, $^3\vec{\text{He}}(\vec{e}, e'p)d$, *and* $^3\vec{\text{He}}(\vec{e}, e'p)pn$ *processes*;
2. JLab experiment E05-015 (co-spokespersons T. Averett, J.-P. Chen, X. Xiang): *Measurement of the target single-spin asymmetry in quasi-elastic* $^3\text{He}^\uparrow(e, e')$;
3. JLab experiment E08-005 (co-spokespersons T. Averett, D. W. Higinbotham, V. Sulkosky): *Target single-spin asymmetry in quasi-elastic* $^3\text{He}^\uparrow(e, e'n)$ *and Measurement of double-spin asymmetries in quasi-elastic* $^3\vec{\text{He}}(\vec{e}, e'n)$;
4. MAMI/A1 experiment, part of Project 'N' (co-spokespersons C. Sfienti, J. Pohodzalla, M. O. Distler): *Triple-polarization asymmetries in* $^3\vec{\text{He}}(\vec{e}, e'\vec{p})$.

1 Physics motivation

The primary motivation to study electron-induced knockout processes involving the ^{3}He nucleus in the initial state and the proton, neutron or deuteron in the final state (see [1] and references therein) is to understand the ground-state structure of this nucleus. This structure is interesting by itself; but it imperative to understand it "well" or "well enough" to be able to interpret all data "on the neutron" for which ^{3}He acts as an effective target. Many fundamental quantities or observables belong to this set, for example the neutron elastic form-factors G_E^n and G_M^n, as well as the polarized quark structure functions corresponding to the neutron, i. e. A_1^n, g_1^n and g_2^n.

2   The JLab E05-102 experiment

The exclusive cross-section for electron-induced deuteron knockout (with both the beam and the target polarized) has the form

$$\frac{d\sigma(h, \vec{S})}{d\Omega_e\, dE_e\, d\Omega_d\, dp_d} = \frac{d\sigma_0}{d\Omega_e\, dE_e\, d\Omega_d\, dp_d} \left[1 + \vec{S} \cdot \vec{A}^0 + h(A_e + \vec{S} \cdot \vec{A}) \right].$$

In the E05-102 experiment [2] we measured two components of $\vec{A}$ (or linear combinations thereof), which correspond to the transverse and longitudinal double-polarization asymmetries

$$A_{x,z} = \frac{[d\sigma_{++} + d\sigma_{--}] - [d\sigma_{+-} + d\sigma_{-+}]}{[d\sigma_{++} + d\sigma_{--}] + [d\sigma_{+-} + d\sigma_{-+}]},$$

where the subscript signs denote the helicities of the electron beam and the orientation of the target spin. The target was polarized along the beam-line and perpendicular to it (in both sideways directions). The asymmetries were measured in and around quasi-elastic kinematics at $Q^2 = 0.25\,(\mathrm{GeV}/c)^2$ for missing momenta up to $270\,\mathrm{MeV}/c$, and compared to the theoretical calculations of the Hannover/Lisbon group [3–6], the Bochum/Krakow group [7–9] and the Pisa group [10].

Neither of the three theories exactly reproduces the measured asymmetries, however, a fair agreement is achieved when a quasi-elastic cut ($\omega < 140\,\mathrm{MeV}$) is applied. This improvement does not come as a surprise since the calculations are known to perform better in the region of the quasi-elastic peak, while their reliability is expected to deteriorate above the peak due to the opening of the pion production threshold and increasing influences of resonances. In short, the asymmetries are in fair agreement with the state-of-the-art calculations in terms of their functional dependencies on p_m and ω, but are systematically offset. For details, see [11].

Similarly, the asymmetries for exclusive processes in which the proton has been knocked out (with obvious modifications to the above formulas) have been measured. These results are being prepared for publication [12].

3   The JLab E05-015 experiment

The motivation of the E05-015 experiment [13] is rather different. It was devoted to the measurement of the single-spin asymmetry in scattering of unpolarized electrons on a transversely polarized ^{3}He target:

$$A_y = \frac{\sigma^\uparrow - \sigma^\downarrow}{\sigma^\uparrow + \sigma^\downarrow}.$$

This asymmetry is proportional to the spin of the target and the cross-product of the incoming and scattered electron momenta, i. e.

$$A_y \propto \mathbf{s} \cdot (\mathbf{k} \times \mathbf{k}').$$

In the Born approximation (single virtual photon exchange, time-reversal invariance) one would expect $A_y = 0$ strictly. Any value $A_y \neq 0$ would be indicative of 2γ-exchange effects which, in turn are proportional to the interference of the one-photon exchange and two-photon exchange amplitudes, $A_y \propto \mathrm{Im}\{T_{1\gamma}T_{2\gamma}^*\}$. Any type of result (null or not) is relevant for the interpretation of proton elastic form-factor determinations and studies of generalized parton distributions. Very limited data on polarized proton exist, but there are absolutely no data of comparable precision on the neutron.

We have measured the single-spin asymmetry in quasi-elastic ^{3}He$^\uparrow(e, e')$ at three beam energies: $E_e = 1.25$, 2.43 and 3.61 GeV and three values of transferred four-momenta $Q^2 = 0.13, 0.46$ and $0.98\,\mathrm{GeV}^2$, respectively. Since $A_y(-\theta) = A_y(\theta)$, the statistics could be doubled by using both Hall A spectrometers simultaneously. We have provided the first measurement of A_y^n (based on extraction from $A_y^{^3\mathrm{He}}$) with an uncertainty several times better than previous proton data. The A_y^n asymmetry is about $-3\,\%$ at the lowest Q^2 and drops in magnitude to about $-1.5\,\%$ at the highest Q^2. The data are presently being prepared for publication [14].

4   The JLab E08-005 experiment

In the JLab E08-005 experiment we have strived to determine the single-spin asymmetries in quasi-elastic ^{3}He$^\uparrow(\vec{e}, e'\mathbf{n})$ process. In contrast to the inclusive process of the E08-005 this is an exclusive reaction and in this particular configuration (transversely polarized target and polarized incoming electrons) the double-polarization asymmetry is a measure of the magnitude of meson-exchange currents and final-state interactions in the neutron knock-out process. The asymmetry should be strictly zero in the plane-wave impulse approximation (PWIA); beyond this approximation, it should die out at high Q^2.

The preliminary results indeed show this trend. The A_y^0 asymmetry drops from approximately 0.7 at the lowest $Q^2 \approx 0.13\,\mathrm{GeV}^2$ to only about a percent at the highest $Q^2 \approx 0.95\,\mathrm{GeV}^2$. On the energy-transfer scale, the measurement span a range from 40 to 120 MeV at $Q^2 \approx 0.13\,\mathrm{GeV}^2$, from 120 to 360 MeV at $Q^2 \approx 0.46\,\mathrm{GeV}^2$, and from 360 to 680 MeV at $Q^2 \approx 0.95\,\mathrm{GeV}^2$.

This experiment also covered the measurement of the corresponding asymmetries in ^{3}He$^\uparrow(\vec{e}, e'n)$, i. e. the same exclusive process but with the target polarized in-plane. (In fact, this data was taken simultaneously with the E05-102 data taking.) Both of these data sets are in the final stage of their analysis and are being prepared for publication [16].

5   The MAMI/A1 triple-polarized $^3\vec{\mathrm{He}}(\vec{e}, e'\vec{p})$ experiment

Is it known [17] that the partial cross-sections σ_L, σ_T and $\sigma_{T'}$ interpreted in terms of PWIA are a means to access spin-dependent momentum distribution of protons and polarized pd-clusters in the ^{3}He nucleus by measuring the asymmetry

$$A = \frac{\mathcal{Y}(1/2, 0, 1/2) - \mathcal{Y}(1/2, 1, -1/2)}{\mathcal{Y}(1/2, 0, 1/2) + \mathcal{Y}(1/2, 1, -1/2)},$$

where

$$\mathcal{Y}\left(M=\frac{1}{2}, M_d=0, \mathfrak{m}=+\frac{1}{2}\right) \propto \left|N_{-1}^{\text{spin PWIA}}\left(\frac{1}{2}, 0, -\frac{1}{2}\right)\right|^2,$$

$$\mathcal{Y}\left(M=\frac{1}{2}, M_d=1, \mathfrak{m}=-\frac{1}{2}\right) \propto \left|N_{+1}^{\text{spin PWIA}}\left(\frac{1}{2}, 1, +\frac{1}{2}\right)\right|^2,$$

and $N_\mu = \left\langle \Psi_{\text{pd}}^{(-)} M_d \mathfrak{m} | \widehat{j}_\mu(\mathbf{q}) | \Psi M \right\rangle$. (It can be shown that $\sigma_L \propto |N_0|^2$, $\sigma_T \propto |N_{+1}|^2 + |N_{-1}|^2$ and $\sigma_{T'} \propto |N_{+1}|^2 - |N_{-1}|^2$.) However, final-state interactions (FSI) and meson-exchange currents (MEC) preclude direct access to them except at $p_d \lesssim 2\,\text{fm}^{-1}$. Still, the investigation of the triple-polarized proton knock-out process has been attempted at Mainz since it allows one to study the rich interplay of final-state wave-function symmetrization, FSI and MEC in specific kinematics. The data have been analyzed [18] and are being prepared for publication.

References

1. S. Širca, Few-Body Systems **47** (2010) 39.
2. S. Širca, S. Gilad, D. W. Higinbotham, W. Korsch, B. E. Norum (spokespersons), *Measurement of A_x and A_z asymmetries in the quasi-elastic* $^3\vec{\text{He}}$ ($\vec{\text{e}}, \text{e}'\text{d}$), JLab Experiment E05-102, June 2005.
3. L. P. Yuan et al., Phys. Rev. C **66** (2002) 054004.
4. A. Deltuva et al., Phys. Rev. C **69** (2004) 034004.
5. A. Deltuva et al., Phys. Rev. C **70** (2004) 034004.
6. A. Deltuva et al., Phys. Rev. C **71** (2005) 054005.
7. J. Golak, R. Skibiński, H. Witała, W. Glöckle, A. Nogga, H. Kamada, Phys. Reports **415** (2005) 89.
8. J. Golak et al., Phys. Rev. C **65** (2002) 064004.
9. J. Golak et al., Phys. Rev. C **72** (2005) 054005.
10. L. E. Marcucci et al., Phys. Rev. C **72** (2005) 014001.
11. M. Mihovilovič et al. (Hall A Collaboration), accepted for publication at Phys. Rev. Lett. (2014).
12. M. Mihovilovič et al. (Hall A Collaboration), in preparation.
13. T. Averett, J.-P. Chen, X. Xiang (co-spokespersons), *Measurement of the target single-spin asymmetry in quasi-elastic* $^3\text{He}^\uparrow$(e, e′), JLab Experiment E05-015, June 2005.
14. Y. Zhang et al. (Hall A Collaboration), in preparation.
15. T. Averett, D. W. Higinbotham, V. Sulkosky (co-spokespersons), *Target single-spin asymmetry in quasi-elastic* $^3\text{He}^\uparrow$(e, e′n) and *Measurement of double-spin asymmetries in quasi-elastic* $^3\vec{\text{He}}$($\vec{\text{e}}$, e′n), JLab experiment E08-005, June 2008.
16. E. Long et al. (Hall A Collaboration), in preparation.
17. J. Golak et al., Phys. Rev. C **65** (2002) 064004.
18. M. Weinriefer, *Untersuchung der Kernstruktur von* ^3He *mittels Polarisationsobservablen*, Doctoral thesis, Johannes-Gutenberg-Universität Mainz, 2011.

Povzetki v slovenščini

Tetrakvarki v limiti kromodinamike z velikim številom barv

Thomas Cohen

Department of Physics, University of Maryland, College Park, MD 20742-4111

Iskanje tetrakvarkov v normalnih in v eksotičnih spektrih še vedno ni prepričljivo, niti eksperimenalno niti teoretično. Podpora pa narašča. Odprto vprašanje je, ali lahko vezani tetrakvarki obstajajo v limiti velikega števila barv. Obstajajo pa na primer v zanimivi antisimetrični varianti kromodinamike.

Sestavljeni šibki bozoni na Velikem hadronskem trkalniku

Harald Fritzsch

Department für Physik, Ludwig-Maximilians-Universität München, Germany

V sestavljenem modelu šibkih bozonov proučujemo vzbujene bozone, zlasti tiste v stanju p. Stanje z najmanjšo maso poistovetimo z bozonom, ki so ga nedavno odkrili na Velikem hadronskem trkalniku v CERNu. Proučujemo značilne lastnosti vzbujenih šibkih bozonov, zlasti njihove razpade v šibke bozone in fotone.

Vpeljava večkvarkovskih interakcij z efektivno Lagrangeovo gostoto

A. A. Osipov, B. Hiller, A. H. Blin

Centro de Física Computacional, Departamento de Física da Universidade de Coimbra, 3004-516 Coimbra, Portugal

Predstavili smo rezultate razširjenega modela Nambuja in Jona-Lasinia s tremi okusi kvarkov. V Lagrangeovo gostoto smo vključili vsa vozlišča brez odvodov, v naslednjem redu razvoja po recipročnem številu barv, za večkvarkovske interakcije s spinom nič. Prikazali smo zlasti vlogo interakcij, ki eksplicitno zlomijo kiralno simetrijo, in njihov učinek primerjali s prejšnjimi modeli.

Kvarkovska snov v močnih magnetnih poljih

Débora Peres Menezes

Universidade Federal de Santa Catarina, Departamento de Física-CFM-CP 476, Campus Universitário-Trindade, CEP 88040-900, Florianópolis-SC, Brazil

V pričujočem prispevku skušamo razumeti razne lastnosti kvarkovske snovi, kot jih opisuje model Nambuja in Jona-Lasinia v prisotnosti močnih magnetnih polj. Najprej analiziramo raznovrstne fazne diagrame. Potem raziskujemo razlike, ki nastanejo zaradi različnih vektorskih interakcij v Lagrangeovi gostoti in uporabimo izsledke za opis zvezdne snovi. Nato se ozremo na značilnosti dekonfinacije in vzpostavitve kiralne simetrije pri kemičnem potencialu nič v okviru prepletene Polyakovove verzije modela Nambuja in Jona-Lasinia. Končno proučimo lego kritične točke za različne izbire kemičnega potenciala in gostote.

Schwinger-Dysonov pristop h kvantni kromodinamiki razloži nastanek oblečenih mas kvarkov

D. Klabučar[a] in D. Kekez[b]

[a] Physics Department, Faculty of Science, Zagreb University, Bijenička c. 32, 10000 Zagreb, Croatia
[b] Rugjer Bošković Institute, Bijenička c. 54, 10000 Zagreb, Croatia

Poleg drugih uspehov Schwinger-Dysonov pristop k neperturbativni kvantni kromodinamiki razloži tudi to, zakaj so v efektivnih kvarkovih modelih oblečene mase kvarkov zelo različne od golih mas. Če pa interakcijsko jedro vsebuje tudi perturbativni delež kromodinamske interakcije, poda Schwinger-Dysonov pristop tudi znano visokoenergijsko obnašanje kvarkovih mas, tako kot jih napoveduje perturbativna kvantna kromodinamika.

Mezonski učinki pri osnovnih in resonančnih stanjih barionov

R. Kleinhappel[a], L. Canton[b], W. Plessas[a] in W. Schweiger[a]

[a] Theoretical Physics, Institute of Physics, University of Graz, Universitätsplatz 5, A-8010 Graz, Austria
[b] Istituto Nazionale di Fisica Nucleare, Via F. Marzolo 8, I-35131 Padova, Italy

Za raziskavo mezonskih učinkov pri osnovnih in resonančnih stanjih barionov smo vključili mezonske zanke v relativistični pristop s sklopljenimi kanali. Iz računov, ki so bili doslej napravljeni na hadronskem nivoju, smo dobili rezultate za oblečene mase osnovnega stanja in resonanc nukleona. S sklopitvijo na pionski kanal smo dobili tudi širine resonanc, zlasti resonance Δ. Za zdaj smo sicer izboljšali rezultate v primerjavi z računi z enim samim kanalom, vendar so razpadne širine še vedno premajhne v primerjavi z meritvami.

Kvarkovski propagator v coulombski umeritvi kvantne kromodinamike

Y. Delgado[a], M. Pak[a], M. Schröck[b]

[a] Institut für Physik, Karl-Franzenz Universität Graz, 8010 Graz, Austria
[b] Istituto Nazionale di Fisica Nucleare (INFN), Sezione di Roma Tre, Rome, Italy

Proučujemo kvarkovski propagator na konfiguracijah gašenega umeritvenega polja v coulombski umeritvi. Pri tem uporabimo kiralno simetrične "prekrivalne fermione". V tej umeritvi lahko povežemo "funkcijo oblačenja" kvarkovskega propagatorja s priporom in kiralno simetrijo kromodinamike. Pripor lahko pripišemo infrardeče divergentni vektorski "funkciji oblačenja". Izvrednotimo "funkcije oblačenja" kvarkovskega propagatorja, razberemo dinamično maso kvarka in ekstrapoliramo vse te količine proti kiralni limiti. Končno razpravljamo, kako se odstranijo nizke Diracove ekscitacije.

Mase oblečenih kvarkov in barionska spektroskopija

W. Plessas

Theoretical Physics, Institute of Physics, University of Graz, A-8010 Graz, Austria

Prikažemo hierarhijo mas oblečenih kvarkov, ki prevladujejo v efektivnih modelih kvantne kromodinamike, zlasti v relativističnem modelu z oblečenimi kvarki. Opazimo, da je presežek dinamično generirane mase nad golo maso bolj ali manj neodvisen od okusa kvarkov in znaša $\Delta m \approx (370 \pm 30)$ MeV. Podobne vrednosti dajo tudi alternativni efektivni opisi barionske spektroskopije, na primer Dyson-Schwingerjev pristop.

Primerjava jedrskih potencialov za hiperon Lambda in za nukleon

Bogdan Povh[a] in Mitja Rosina[b,c]

[a] Max-Planck-Institut für Kernphysik, Postfach 103980, D-69029 Heidelberg, Germany
[b] Fakulteta za matematiko in fiziko, Univerza v Ljubljani, Jadranska 19, p.p.2964, 1001 Ljubljana, Slovenija
[c] Institut J. Stefan, 1000 Ljubljana, Slovenija

Raziskujeva verjetni mehanizem, zakaj čuti hiperon Λ dvakrat šibkejše jedrsko polje (okrog -27 MeV) kot nukleon (okrog -50 MeV).

Izbrani spektroskopski rezultati kolaboracije Belle

Marko Bračko[a,b]

[a] University of Maribor, Smetanova ulica 17, SI-2000 Maribor, Slovenia
[b] Jožef Stefan Institute, Jamova cesta 39, SI-1000 Ljubljana, Slovenia

V prispevku smo poročali o izbranih rezultatih iz spektroskopskih eksperimentov, pred kratkim izvedenih s spektrometrom Belle, ki deluje na energijsko asimetričnem trkalniku elektronov in pozitronov KEKB v laboratoriju KEK, Tsukuba, Japonska.

Konstituentni kvark kot soliton v kiralnih kvarkovskih modelih

Bojan Golli

Pedagoška fakulteta, Univerza v Ljubljani, 1000 Ljubljana in Institut Jožef Stefan, 1000 Ljubljana, Slovenija

Obravnavamo možnost, da lahko soliton z barionskim številom 1/3, dobljenim v linearnem modelu sigma in v modelu Nambuja in Jona-Lasinija, identificiramo s konstituentnim kvarkom. V linearnem modelu sigma smo izpeljali potencial med dvema solitonoma, ki je podoben potencialom, ki se uporabljajo v modelih s konstituentnimi kvarki.

Mezoni D_s s pozitivno parnostjo in Z_c^+ v kromodinamiki na mreži

Luka Leskovec

Institut Jožef Stefan, Jamova 39, 1000 Ljubljana, Slovenija

Predstavljena sta dva še posebej zanimiva kanala: D_s mezoni s pozitivno parnostjo ter eksotični hadron Z_c^+. V kanalu z D_s je bilo nekaj napetosti med eksperimentom ter teorijo, saj je eksperiment našel stanji $D_{s0}^*(2317)$ in $D_{s1}(2460)$ pod pragom za sipanje mezonov DK in D^*K, medtem ko je teorija napovedala mase teh mezonov nad tem istim pragom. V kromodinamiki na mreži smo simulirali dotični kanal tako, da smo uporabili operatorje $\bar{c}s$ ter tudi $D^{(*)}K$. Upoštevajoč pojave na pragu sipanja smo izločili mase mezonov D_s s pozitivno parnostjo, ki se nahajajo pod pragom za sipanje in se v okviru napak ujemajo z eksperimentalnimi. Simulirali pa smo tudi eksotični kanal v katerem se nahaja Z_c^+. Uporabili smo vse relevantne dvomezonske sipalne operatorje $J/\psi\pi, \eta_c\rho$, DD^*, $\psi(2S)\pi$, D^*D^*, $\psi(3770)\pi$, $\psi_{3^{--}}\pi$, kot tudi dodatne operatorje tipa dikvark anti-dikvark. Identificirali smo vse diskretne energijske nivoje, a nismo našli prepoznavnega kandidata za Z_c^+.

Primerjava mas oblečenih in golih kvarkov

Mitja Rosina

Fakulteta za matematiko in fiziko, Univerza v Ljubljani, Jadranska 19, p.p.2964, 1001 Ljubljana, Slovenija
in Institut J. Stefan, 1000 Ljubljana, Slovenija

Zelo zanimivo je, da je razlika med golo maso in oblečeno maso (kot jo uporabljamo v efektivnih kvarkovih modelih) skoraj konstantna od lahkih do težkih kvarkov. Znaša 330 MeV za kvarke u in d in naraste na 400 MeV (ali 600 MeV) za težje kvarke. Masa oblečenih kvarkov je seveda odvisna od modela. Za kvalitativno razumevanje, kateri mehanizmi prevladujejo v raznih modelih, si ogledamo kromodielektrični model, linearni sigma model ter model Nambuja in Jona-Lasinia.

Raziskave spinske strukture ^{3}He v procesih izbijanja devterona in nukleonov

Simon Širca[a,b]

[a] Fakulteta za matematiko in fiziko, Univerza v Ljubljani, Jadranska 19, 1000 Ljubljana
[b] Jožef Stefan Institute, Jamova 39, 1000 Ljubljana

V predavanju sem predstavil statusno poročilo o nekaterih eksperimentih, ki so bili pred kratkim izvedeni v okviru kolaboracije Hall A laboratorija Thomas Jefferson National Accelerator Facility (TJNAF) oz. Jefferson Lab (JLab) in v okviru kolaboracije A1 pri pospeševalniku MAMI (Mainz, Nemčija). Skupni imenovalec vseh teh prizadevanj je študij strukture jedra ^{3}He v osnovnem stanju.